HERON contains contributions based mainly on research work performed in I.B.B.C. and STEVIN and related to strength of materials and structures and materials science.

Jointly edited by:

STEVIN-LABORATORY
of the Department of
Civil Engineering of the
Delft University of Technology,
Delft, The Netherlands
and
I.B.B.C. INSTITUTE TNO
for Building Materials
and Building Structures,
Rijswijk (ZH), The Netherlands.

EDITORIAL BOARD:
J. Witteveen, *editor in chief*
G. J. van Alphen
M. Dragosavić
H. W. Reinhardt
A. C. W. M. Vrouwenvelder
L. van Zetten

Secretary:
G. J. van Alphen
Stevinweg 1
P.O. Box 5048
2600 GA Delft, The Netherlands
Tel. 0031-15-785919
Telex 38070 BITHD

HERON vol. 26
1981
no. 1c

Contents

NUMERICAL MODELS FOR REINFORCED CONCRETE STRUCTURES IN PLANE STRESS

H. J. Grootenboer [1]
S. F. C. H. Leijten [2]
J. Blaauwendraad [3]

[1] TH-Twente University of Technology (WB)
Postbox 217 - 7500 AE Enschede
[2] S.I.P.M. - Holland
Postbox 162 - 2501 AN The Hague
[3] Rijkswaterstaat Bouwresearch
Postbox 20000 - 3502 LA Utrecht

CUR VB

This publication has been issued in close co-operation with the Netherlands Committee for Research, Codes and Specifications for Concrete (CUR-VB).

Publications in HERON since 1970

LIST OF SYMBOLS

A	area of cross-section
A_e	area of element
B	rigidity of boundary layer with respect to widening
D	dowel rigidity; initial modulus of elasticity (matrix)
E	modulus of elasticity
E^s	secant modulus of elasticity
F	load; normal force in reinforcing element
G	shear modulus
H	hardening function
J_1, J_2	stress invariants
K	viscous stiffness; rigidity of boundary layer with respect to parallel displacement
L	interpolation function for boundary displacements
P_1, P_2	interpolation function for stresses
S	stiffness matrix; yielding force for damper; shear force in reinforcement element
S_A, S_B	stiffness matrices after cracking
a_0	stress at which concrete starts yielding and hardening
b	width of beam
e_{xx}	axial strain in beam
e_{yy}	strain in stirrups
f_b	bond strength at which slip starts
f_y	yield strength of steel
f_c	compressive strength of concrete
f_{ct}	tensile strength of concrete
f_d	strength of concrete for dowel action
h	depth of beam
k	constant for aggregate interlock; global load vector
k_A, k_B	global load vectors after cracking
$k_{\varepsilon_1}, k_{\varepsilon_1}$	global load vectors due to initial strains
$k_{\beta_2}, k_{v_A^0}$	global load vectors due to additional stress parameters β_2 and displacements v_A^0
q_x, q_y	distributed surface loads
t	time
$u, \bar{u}$	displacement component
$v, \bar{v}$	displacement component; vector of displacements
v^0	global vector of displacements
v_A^0, v_B^0	global vector of displacements after cracking
w	displacement component
α	angle in crushing envelope for concrete; multiplication factor for shear modulus

β_1, β_2	vectors of stress parameters
γ, γ_{xy}	shear deformation
ε	axial strain
ε^I	initial strain
ε^p	plastic strain
$\bar{\varepsilon}^p$	equivalent plastic strain
$\varepsilon^p_{\max}, \bar{\varepsilon}^p_{\max}$	maximum (equivalent) plastic strain
ε_{vp}	strain in viscous damper
$\varepsilon_{11}, \varepsilon_{22}$	principal strains
ε_s	shrinkage deformation
ε_{bs}	basic shrinkage deformation
$\varepsilon_{\text{creep}}$	creep strain
φ	displacement component; final value of creep
κ_{xx}	curvature of beam
ν	Poisson's ratio
ν^s	secant value of Poisson's ratio
σ	normal stress in bond layer and in aggregate interlock layer
$\bar{\sigma}$	equivalent stress
$\sigma_{xx}, \sigma_{yy}, \sigma_{xy}, \sigma_{yx}$	stresses in concrete
σ_s	stress in steel; maximal normal stress for dowel forces
σ_{11}, σ_{22}	principal stresses
τ	parallel stress in bond layer and aggregate interlock layer
ω	measure for amount of stirrup reinforcement
$\Delta_\perp, \Delta_{/\!/}$	relative displacement in bond layer and in aggregate interlock layer

Preface

This issue of HERON contains the theoretical and numerical results of a research project on mathematical models for the analysis of reinforced concrete structures, which has been carried out at Rijkswaterstaat (State Public Works) in the Netherlands. This project is part of the joint project "Betonmechanica" (Concrete Mechanics) which is being conducted by Rijkswaterstaat, TNO-IBBC (Institute TNO for Building Materials and Building Structures) and the two Universities of Technology at Eindhoven and Delft, respectively. The whole project has been split up into four separate projects, some of which consist of two parts in themselves. The following diagram shows the (parts of the) four separate projects and their interrelations [1].

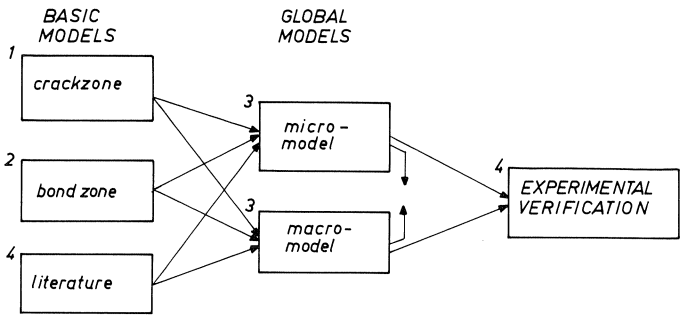

The projects 1, 2 and 4 concern what we call the basic modelling of cracks, bond, etc. They are being carried out by specialists on concrete research. The results of the projects 1 and 2 on the basic modelling of cracks and bond have been published in the HERON issues 1981, 1a and 1b [2, 3]. These results are input for project 3 in which the basic models are used to describe the global behaviour of a structure. In this third project two computer programs have been derived, the Micro-model and the Macro-model. These models were developed by specialists on numerical methods in engineering mechanics.

The object of this approach was to concentrate on the investigation of basic components in the behaviour of reinforced concrete structures, to model the behaviour of these basic components and to incorporate these basic models in the global models. With those global models reinforced concrete structures could be studied, thus increasing the fundamental knowledge of the behaviour of reinforced concrete. More detailed information about the objectives of the "Betonmechanica" project and the division into four projects can be found in the workplan and survey of the joint project [1].

The joint project is being supervised and partly financed by the CUR-VB (Netherlands Committee for Research, Codes and Specifications for Concrete), which has set up the Working committee A26 "Betonmechanica". The authors are indebted to the members of this committee for their contributions, help and encouragement.

The theoretical work for the Micro-model was done by dr. ir. H. J. Grootenboer (Bridges Department of Rijkswaterstaat). Mr. P. J. G. Merks (Bridges Department of Rijkswaterstaat) was very helpful in testing the program, performing the many calculations and preparing the several documents which describe the program.

The basis for the Macro-model was initially laid down by dr. ir. J. Blaauwendraad (Data Processing Division of Rijkswaterstaat), and ir. S. F. C. H. Leijten (Data Processing Division of Rijkswaterstaat) realized the program in its recent final form. Mr. R. H. de Meijer (Bridges Department of Rijkswaterstaat) helped in testing the program and carried out a number of calculations. Ir. J. van Mier of the University of Technology at Eindhoven undertook to do a parameter study using the program. The project leader for the overall work of both the Micro-model and the Macro-model was dr. ir. J. Blaauwendraad.

This publication can be regarded as a comprehensive summary of all the results. A detailed account of the theory is given in the following reports.

1. GROOTENBOER, H. J., Finite element analysis of twodimensional reinforced concrete structures, taking account of nonlinear physical behaviour and the development of discrete cracks, Doctoral Thesis, Delft University of Technology, The Netherlands, March 1979 [4].
2. LEIJTEN, S. F. C. H. and J. BLAAUWENDRAAD, Stanil/1, a macro-beam-model for the nonlinear analysis of reinforced concrete plane frames, Rijkswaterstaat, February 1981 [5].

NUMERICAL MODELS FOR REINFORCED CONCRETE STRUCTURES IN PLANE STRESS

Summary

This issue of HERON reports the development of two numerical models for the analysis of reinforced concrete structures in plane stress. In the PREFACE it is explained how this project fits into a joint project named "Betonmechanica" in the Netherlands.

In an introductory chapter the motives for this study are outlined and the essentials of reinforced concrete structures are reviewed. This survey indicates the need for analysis, which led to the decision to derive a Micro-model and a Macro-model.

Micro-model

The Micro-model is a progam based on a special type of finite element method for plates in plane stress. Material nonlinearities can be dealt with, but geometrical nonlinearity has not been taken into account. Bond and bond slip are modelled. Probably a feature which attracts most attention is the possibility of having discrete cracks across elements in any direction. This makes the program particularly well suited to simulate structures which fail in a brittle mode in which one crack or just a few cracks dominate their behaviour. The program is called MICRO/1.

Its scope is discussed in Chapter 2 and an outline in the theory is presented in Chapter 3. The program will mainly be used in a research context for the investigation of special types of structures and details. Examples of the verification of the model, which are intended to illustrate the field of applications, are given in Chapter 4. This part ends with some conclusions and a survey of possible work ahead.

Macro-model

The Macro-model is a program for plane beams and framed structures. Material nonlinearities as well as geometrical nonlinearities are dealt with. In this program the concept of "smeared-out" cracks is applied. Only bond and bond slip between the main reinforcing bars and the concrete are modelled. The aim of the program is to calculate the global behaviour of a beam up to failure load, rather than to study detailed stresses as in the case of the Micro-model. The Macro-model program is called MACRO/1.

The scope of this model is described in Chapter 6, and the theory applied is outlined in Chapter 7. Examples of analysis to verify the possibilities of the model and to illustrate the range of application are presented in Chapter 8. Finally conclusions and indications for work ahead are given in Chapter 9.

Numerical models for reinforced concrete structures in plane stress

1 Introduction

1.1 *Motives*

In the course of this century the material called concrete, reinforced or prestressed with steel, has become one of the most important building materials in civil and structural engineering. The design and execution of new structures which – in respect of shape, method of construction or manner of loading – are outside the range of standard experience make it continually necessary to investigate the behaviour of concrete structures.

Examples of such structures are: offshore structures, nuclear power stations, and water engineering structures in or closely associated with the sea, such as the surge tide barrier in the Eastern Scheldt (Oosterschelde).

Increase in dimensional scale and the introduction of new techniques in the building of bridges and tunnels, however, also necessitate further research. In addition, the rise in cost of all types of structure makes it essential to go on seeking less expensive alternative designs, materials and construction methods without lowering of safety standards.

Closely bound up with scale increase is the corresponding increase in the seriousness of the consequences of disaster, so that careful and detailed structural safety analysis becomes more and more necessary. The central feature of such an analysis is an investigation of the loading and of the behaviour of the structure under all kinds of conditions such as cyclic loading (alternating loads), its time-dependent behaviour and especially its behaviour under overloading.

Investigation of the behaviour of concrete structures has hitherto chiefly been based on the results of tests performed on model structures or on structural components in the laboratory. Such tests provide good insight in the deformation of the structure and the magnitude of its failure load. But they yield only limited information on the strains and relative displacements of the embedded steel. Because of this, the interpretation of the behaviour and the detection of the causes thereof are made much more difficult.

Knowledge of the causes of a certain behaviour is important in order to predict the behaviour of other structures or of similar structures under different loads.

The possibilities of mathematically predicting the behaviour of a concrete structure have been greatly extended as a result of the development of the computer. What are needed, besides a numerical model for describing the structure, are mathematical models embodying our knowledge of the behaviour of the constituent materials (steel and concrete) and of their manner of cooperation. One important condition for the attainment of an optimum result is the collaboration of investigators in these two fields of research, namely numerical methods in engineering mechanics, on the one hand, and fundamental research of reinforced concrete on the other. In the project "Betonmechanica" this condition has been met.

1.2 *Essentials of reinforced concrete structures*

The behaviour of the material reinforced concrete is particularly complex. This is apparent from the following points:

- The maximum tensile stress that concrete can resist is much less than the maximum compressive stress that it can resist.
- The relation between compressive stress and strain deviates already at a relatively low level of stress from the linear relation in accordance with Hooke's law. Besides, this compressive strain is dependent not only on the stress acting at any particular instant, but also on the previous history of the stress.
- Concrete shrinks and swells. The magnitude and rate of these phenomena depend on, among other factors, the humidity of the environment and the dimensions of the structure.
- The creep deformation of concrete is considerable and may be as much as three times the elastic deformation. On removal of load, part of the creep is recoverable and part of it is irrecoverable.
- If a crack develops in concrete, transfer of shear forces across the crack nevertheless continues to be possible because the faces of the crack are not smooth, so that the irregularities on them will interlock if the width of the crack is small (aggregate interlock). The magnitude of the maximum shear that can thus be transferred across a crack depends on the width of the latter.
- The bond between the steel reinforcement bar and the surrounding concrete is not perfect. For low load levels the connection behaves as a linear spring, but for higher loads nonlinear behaviour may occur and even slip of the bar relative to the concrete.
- The anchoring zone of a rebar represents a complex problem, which essentially is a three-dimensional stress state.

To compensate for its low tensile strength, concrete is reinforced with steel bars and/or prestressed with tendons (high-tensile steel wires or bars).

In the composite material formed in this way the steel, by virtue of its quality and shape, largely determines the cooperation of the two materials. Bond between concrete and steel, slip of the reinforcement and plastic deformation of the steel are important aspects with regard to this. In an unreinforced concrete structure, cracks develop already at low values of the loading. Cracks may considerably reduce the stiffness of the structure. When they are formed, the internal stress distribution is greatly changed. The reinforcing steel, which in the uncracked structure contributes only little to the actual loadbearing capacity, is now loaded to a high stress, as are also the contact surfaces between the steel and the concrete. The cooperation of the two materials now depends greatly on the quality of their bond and on the dowel action of the reinforcement at a crack in the concrete. The directions of the reinforcement and of the cracks have a major effect on the anisotropic behaviour of the cracked composite material.

Failure of a reinforced concrete structure may result from the occurrence of large deformations and thus exhibit a "ductile" character. Alternatively, however it may be of a "brittle" character. This last-mentioned form of failure can be particularly dangerous

because it is not initiated by large crack widths or deflections. In that case, too, the possibility of redistribution of forces which exists in a statically indeterminate structure cannot be utilized sufficiently.

1.3 *Analysis needs*

Calculations for the design and analysis of reinforced concrete and prestressed concrete structures are usually based on linear elastic theory. This approach takes no account of the non-linear behaviour of the constituent materials, the reduction in stiffness due to cracking and the transition from isotropic to anisotropic properties for the composite material. Such calculations can therefore only provide insight into the behaviour of a structure at low values of loading. This is not necessarily a disadvantage with regard to structures within the conventional range of experience. The codes of practice often contain design rules to ensure that structures continue to conform to the relevant safety requirements also at higher loads.

A different situation exists with regard to new types of structures for which experience is as yet lacking. In most cases there are no codes or established design rules for them, and to test a prototype is often impracticable. For designing such structures and assessing their safety it is essential to have information on their behaviour under loads of large magnitude up to and including failure load.

Since this behaviour is to a great extent determined by the above-mentioned non-linear behaviour of the materials, the analysis of these structures has to be based on models which take this behaviour into account. The calculations do indeed become much more complex in consequence of this and practically impossible to perform without the aid of a computer. The evolution that non-linear analysis models for reinforced concrete structures have undergone in the period from 1967 to the present time is considerable. All the models developed in this time are based in the finite element method, because this numerical technique has proved to be particularly suitable for solving many kind of problems in structural analysis with the aid of a computer. In the work of all the investigators in this field the emphasis is on the treatment of cracking. This is not surprising, since crack formation is of major influence on the stiffness, the internal stress distribution and the maximum loadbearing capacity of the structure. The first investigators to include cracking in their model were Ngo and Scordelis. In their analysis of reinforced concrete beams they took account of the cracks by detaching the elements at their boundaries.

This schematization of cracking was later also used by Nilson and by Stauder et al. In this method a crack is treated as a line on either side of which the displacements may differ in magnitude. This model offers the advantages that the displacements at a crack can be calculated and that these displacements can be taken into account in determining effects such as aggregate interlock, dowel forces and yielding of the reinforcement. This model nevertheless was abandoned, the reasons for this being:

- the limitation that cracks can occur only along the element boundaries. This results in a high degree of schematization of the cracking pattern and considerable depen-

dence on the subdivision into elements.

- the second drawback relates to the method of analysis. In consequence of the detachment of the elements the system of equations must each time be established afresh and inverted or decomposed. In addition, the altered number of degrees of freedom has to be taken into account.

In general, the discrete crack model has been abandoned in favour of the approach in which a crack is smeared or spread out over a whole element or over part of an element. The crack is thus incorporated into the stiffness properties of the concrete, which becomes anisotropic in consequence. The crack directions determine the principal direction of this anisotropy.

One of the first investigators to use this method for the analysis of plates was Franklin. Its great advantage is that cracking is conceived as a phenomenon like plastic deformation and can therefore be analysed by the same methods, with which a good deal of experience has already been gained. In this way, it becomes also possible to use standard programs for the analysis of reinforced concrete structures.

The disadvantages of this method are due to "smearing out" the cracks. It is thus not possible to deal with displacements at the cracks in the aspects already mentioned, namely, aggregate interlock, dowel action and yielding of the steel. With this model the crack spacings and crack widths are difficult to calculate, even if a fine-meshed network of elements is used. Whether these drawbacks constitute a serious objection will depend on the kind of structure to be analysed. Experience shows that structures in which the bending moment is the determining quantity with regard to loadbearing capacity (ultimate strength) and which have a ductile load-deformation diagram, can very suitably be analysed with these models. On the other hand, structures displaying brittle failure behaviour, which is frequently determined by one or a few dominant cracks, are not so suitably amenable to analysis on the basis of this model with "smeared-out" cracks. This frequently relates to shear cracks or flexural cracks in short cantilevers and comparable other structures.

Another facet to which attention is paid in the work of many investigators, is the mathematical modelling of bond. Not all of them adopt the same manner of schematization for the reinforcement. In those models that are based on discrete cracks the bars are always described with the aid of separate elements. These reinforcement elements are in many instances connected to the concrete elements by springs. The latter represent the behaviour at the boundary layer between steel and concrete. With this schematization it is possible to take proper account of the slip of the reinforcement in the concrete when the shear stresses between the bar and the concrete have attained a maximum value.

In the models with "smeared-out" cracks the reinforcement is often incorporated into the properties of the plate element. For this element the aeolotropic properties of the composite material comprising concrete plus steel are then introduced into the analysis. In that case, however, one usually does not take account of displacement of the steel bar in relation to the concrete (slip).

Apart from the decision as to which method is chosen to represent the crack pheno-

menon and the bond behaviour, it is always a difficult choice which model should be preferred to describe the behaviour of plain concrete under two-dimensional and three-dimensional states of stress.

A number of them can be found in literature. The results obtained with these respective models often differ considerably from one another, the reason being that as yet not enough is known concerning this behaviour.

The knowledge which has existed also with regard to the shear transfer behaviour at a crack (aggregate interlock) has been appreciably increased by the results of project 1 of "Betonmechanica". These results of theoretical and experimental studies concerning the behaviour of the cracked zone are dealt with in the issue of HERON, 1981, No. 1a.

For the behaviour of the boundary layer between steel and concrete (bond), fresh information can be obtained from the results of project 2 of "Betonmechanica". This will be the subject of HERON, 1981, No. 1b.

Having discussed the choice between inter-element discrete cracks and smeared-out cracks, the possibilities to incorporate bond in the model and the recent status of material constitutive laws, we can state the *needs* for improvement. It will be a major step forward to derive a fine-scale numerical model which allows for the occurrence of discrete cracks at (preferably), any position within an element. This model has to include bond behaviour, dowel action, aggregate interlock, creep, shrinkage and swell, and a generally applicable nonlinear constitutive law for plain concrete. It is obvious that such a fine-scale program will be expensive in use because of the consumption of much core and computing time of a computer. Therefore such å program can only be used for research and for examining structural details. For complete structures we need a separate program which takes account of the most important essentials of reinforced concrete without going into too detailed an analysis of the structure. In the context of the project reported here one should think of a program for frames. The approach based on smeared-out cracks will then serve the purpose, and the bond is only modelled along the main reinforcement and not along the stirrups.

1.4 *Micro-model and Macro-model*

The requirements formulated in section 1.3 have been met in developing two programs, which we have designated the Micro-model and the Macro-model. Both numerical models are finite element models.

Micro-model

In the micro-model the physical phenomena of crack propagation, transfer of stresses across cracks, bond stresses, etc. are described very realistically. The micro-model aims at increasing the fundamental knowledge of the behaviour of reinforced concrete structures.

First and foremost in connection with the development of the Micro-model was the desire to devise a model with which the behaviour of a structure can be analysed under various loads, enabling both the overall behaviour (e.g., a load-deflection diagram or a

moment-curvature diagram for a portion of a beam) and the local occurrences within the structure to be described. The aim is to devise an instrument which can take the place of very expensive laboratory tests (with much internal recording of data) or which can assist in the interpretation of laboratory measurements with a limited number of recorded data. Of particular interest is the behaviour after the occurrence of the first cracks and on attainment of the failure load. The model must be able to indicate the failure load, the cause of failure and the deformations that occur. In reinforced concrete structures the collapse mechanism is determined by the system of cracks that develops in the concrete, and the collapse load or, more generally, the failure load will depend on the stresses in the concrete and steel in the vicinity of the cracks.

Of special interest are those problems in which the structure, on reaching the failure load, displays brittle behaviour. Such behaviour occurs in failure due to shear or to a combination of shear and bending.

In these types of failure the dowel action of the reinforcement and the transfer of shear stresses at a crack play a major part. The deformation of the structure on attainment of the failure load will, in such cases, depend to a great extent on the slip of the reinforcement and the deformations of the concrete. Brittle failure of a structure is often the result of one dominant crack. The displacements at that crack determine the above-mentioned dowel forces, the shear stresses at the crack and the steel stresses in the vicinity of the crack.

It was endeavoured to find a model with discrete cracks, because in this way the displacement at a crack can suitably be determined and the effects of these displacements on the internal stresses can be taken into account. Also, this model can be expected to make the dominant crack distinctly discernible.

The new program has been written as a subsystem of the general engineering system Genesys. The name of this subsystem is MICRO/1. So the names Micro-model and MICRO/1 may be used for the same program.

Macro-model

Apart from fundamental knowledge, designers wish to have a tool to investigate total (marginal) structures. As already stated, the fine-scale Micro-model may be expected to produce information that is too detailed for such operational problems and may cost a lot of money. Therefore a rough-scale numerical model, in short: the Macro-model, was developed at the same time. This program can be regarded as a new extended version of an existing program, called STANIL, for plane framed structures (the name of the program is a contraction of three Dutch words: STAaf = bar, NIet-Lineair = non-linear). The STANIL program had been developed in earlier years by Rijkswaterstaat and TNO-IBBC. The now rewritten program is a subsystem of Genesys and has been named STANIL/1. So the names Macro-model and STANIL/1 may be used for the same program. This rough-scale model aims at describing the behaviour of reinforced concrete structures in a macro sense. In this model it is sufficient to use averaged values of stiffnesses (due to smeared-out cracks). Large beam-type elements are used.

MICRO-MODEL

2 Scope of Micro-model

The Genesys subsystem MICRO/1 is a program for the advanced analysis of two-dimensional plane structures of reinforced concrete, e.g. walls, a detail like a beam-column connection and so on. The structures are assumed to display nonlinear elastic behaviour and to be statically loaded. Only material non-linearity is considered. Creep, shrinkage and temperature changes can be dealt with. The program produces plots of cracks after each load increment which allows the crack propagation to be studied. Of course, stresses, displacements and support reactions also occur in the output. The width of all individual cracks is likewise calculated.

The shape of the plane structure may be arbitrary in the sense that the element mesh consists of triangular concrete elements and straight reinforcing bar elements.

In the micro-model a method of crack schematization is adopted which combines the advantages of discrete cracks and of the approach based on smeared-out cracks. The cracks are treated as (what they in reality are) discrete material boundaries, for which the displacements and the normal stresses in the crack direction may be different on both sides. These discrete cracks may pass through the element mesh at any place in any direction, and they are continuous over the element boundaries. Furthermore, the various types of non-linear material time-independent and time-dependent behaviour are considered in the model. Reinforcing bars may occur on the interface of two elements; so they never cross a single element. A boundary layer for the bond phenomenon is adopted between each bar and the neighbouring concrete elements.

Type of finite element method

A special type of the finite element method is applied. In deriving the triangular thin plate elements for the plane state of stress in the concrete the concept of "natural boundary displacement" is used, as was introduced by Blaauwendraad [6]. Instead of degrees of freedom at the corner, separate sets of degrees of freedom have been introduced for each of the three element edges. So the displacements at one edge are completely disconnected from the displacements of another edge in the same element. Such elements show stresses at their boundaries which are always in equilibrium with one another and with the internal loading. The stiffness matrix of such elements is derived from an assumed field of stresses over the internal element area and an assumed displacement distribution along the element boundaries (hybrid method).

It was considered that the freedom to choose a stress field offered the most promising possibilities to describe the complex state of stress in an element crossed by a crack.

Possibilities and restrictions of MICRO/1

Applications of the MICRO/1 program are found in investigating:

- cracks and stresses in wall-type structures;
- details of structures such as beam-column connections;
- the ultimate bearing capacity of beams and columns under combined states of normal force, bending moment and shear force; especially failure in shear can now be studied;
- all crack problems in which crack spacing and crack width are of particular interest;
- typical (details of) structures in which the overall behaviour is strongly dependent on the bond characteristics.

It has to be stated here, however, that some types of problem cannot be properly modelled. MICRO/1 has, for instance, not been built for the investigation of three-dimensional stress states. This means that the anchoring zone of reinforcing bars cannot be examined precisely. And, in general, each circular bend in a bar is schematized by a sharp angle. So one should be careful in these cases.

Some of the facilities that the now available program MICRO/1 offers are (besides those already mentioned above):

- the structure supports may be springs;
- dependence relations between degrees of freedom can be stated;
- the tensile strength can be chosen according to a random distribution over the several elements;
- users can choose between two different constitutive laws for the concrete.

A separate program PLAAT/1 has been built for plates in bending, which to a great extent is similar to the progam MICRO/1. This program for plate bending officially does not belong to the "Betonmechanica" project and will therefore not be reported in this publication.

Integration of basic models and global models

It was indicated in the Preface that the intention of the "Betonmechanica" project is to incorporate the basic models from the other projects in the global models. In order not to delay the development of the global models, preliminary choices had to be made for the basic models based on what was known from the literature. The integration of the results of the other projects in MICRO/1 has been scheduled at the time of preparing this report. It may be published in a future issue of HERON.

Survey of contents

An outline of the basic considerations which led to the micro-model and theory will be given in Chapter 3. It has been decided not to go into much detail, but to provide sufficient information for understanding the essentials of MICRO/1. So the derivation of the stiffness matrix of the triangular element for the concrete is not fully described; neither the manner in which the global nonlinear equations were formed has been explained in detail. In Chapter 4 the reader will find a number of applications which clarify the potentialities of this new numerical tool in advanced mechanics.

3 Outline of theory of Micro-model

3.1 *Physical phenomena to be modelled, and schematization of geometry*

The structure is modelled with triangular elements of concrete and linear elements of reinforcement (Fig. 3.1). Where reinforcing bars occur the material is concentrated at the central line and the joining concrete elements are assumed to extend up to this central line of the reinforcement.

The reinforcement will in general display displacements relative to the surrounding concrete. Around the steel bar there is a boundary layer in which the bond phenomenon takes place. Fig. 3.2 shows which cracks really may occur in this region and how it is idealized to a homogeneous axisymmetric layer. The layer transmits a shear stress τ from the concrete to the bar. The deformation of the layer due to this shear force is greatly influenced by the radial stress σ. The dimensions of the layer can be neglected in the finite element mesh (as can be done for the bars), but the stiffness relation between the stresses τ and σ on the one hand and the corresponding deformations of the layer on the other hand should be considered.

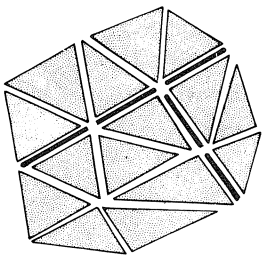

Fig. 3.1. Illustration of assembly of triangular concrete elements and straight bar elements.

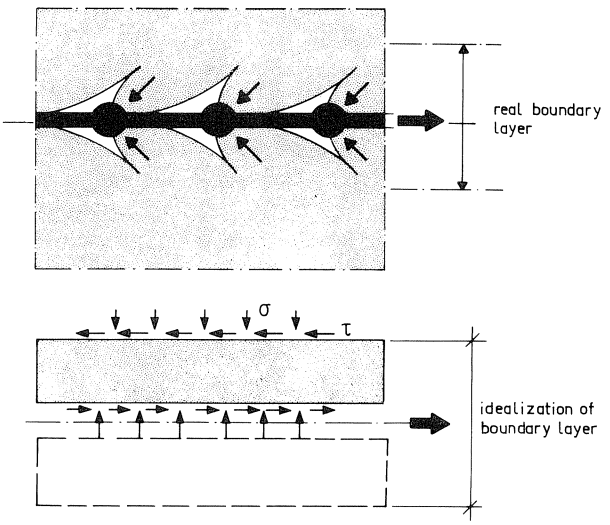

Fig. 3.2. Real situation in a boundary layer for bond and its idealization.

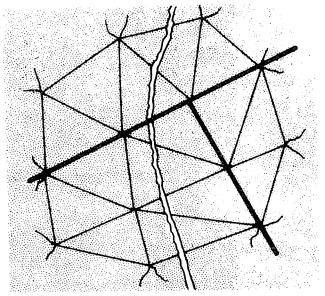

Fig. 3.3. Cracks should be allowed to develop irrespective of the chosen element mesh.

The next phenomenon to be dealt with is cracking. We wish to allow the occurrence of cracks irrespective of the choice of the element mesh (Fig. 3.3.).

In a crack, aggregate interlock takes place. This means that force transfer is still possible after cracking, but this is accompanied by displacements of the two crack faces relative to each other, parallel to the crack and also perpendicular to the crack (Fig. 3.4).

The crack zone behaviour is schematized as the behaviour of a homogeneous layer between the two crack faces. In this layer (average) stresses τ and σ occur, which cause deformations of the layer corresponding to the parallel displacement of the crack faces and the perpendicular displacement (the crack width). In the finite element mesh the

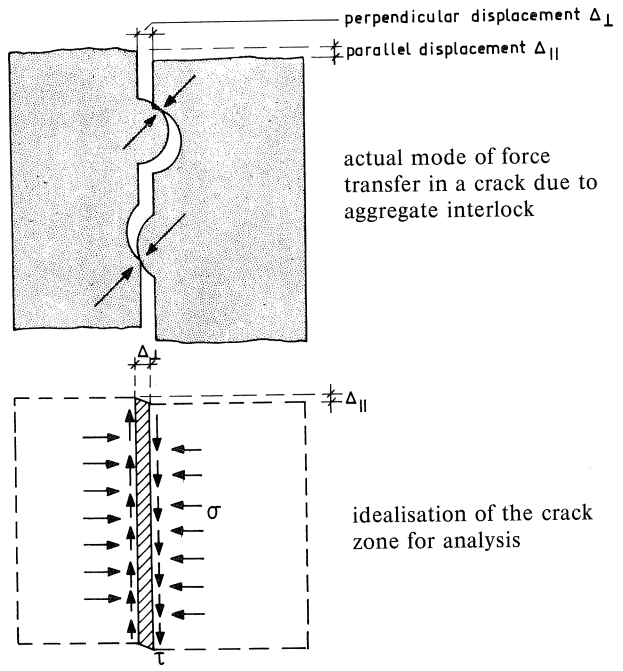

Fig. 3.4. Real aggregate interlock in the crack zone and the idealization of the zone.

two crack faces can be assumed to have the same geometrical position, so we neglect the dimensions of the crack zone layer (as is done with the bond layer). But the stiffness relation between the stresses and the corresponding relative displacements of the crack zone layer should be taken into account.

The proposed crack zone layer implies that the shear stress and the stress normal to the crack are continuous across a crack. Note that the stress normal to the crack need not be zero in this concept, as is normally assumed for cracks. This assumption holds exactly only if no parallel displacement occurs. In the case of parallel displacements the assumption is still fairly good for very small crack widths and for large crack widths. For intermediate values of the crack width the normal stress and the shear stress in the crack may have the same order of magnitude. The normal stress parallel to the crack need not have the same value in the concrete on one side and in the concrete on the other side of the crack. The analysis should allow for this discontinuity in stress across a crack.

Finally, consider the situation of a crack crossing a reinforcing bar. In that position two aspects must be considered: firstly, an abrupt change of the sign of the bond shear stress and, secondly, dowel action. Fig. 3.5 shows the type of shear stress distribution that can be expected along the reinforcement near a crack in a tensile region. The analysis should take account of this, if not the exact distribution of the stresses, at least the discontinuity at the crack must be accounted for.

Fig. 3.6 shows the deformation of a reinforcing bar when a parallel displacement occurs in a crack. The bar behaves like a dowel, with high normal stresses transmitted between the concrete and the bar. In this region the bar can be conceived as a bar loaded in bending wich is supported by an elastic foundation.

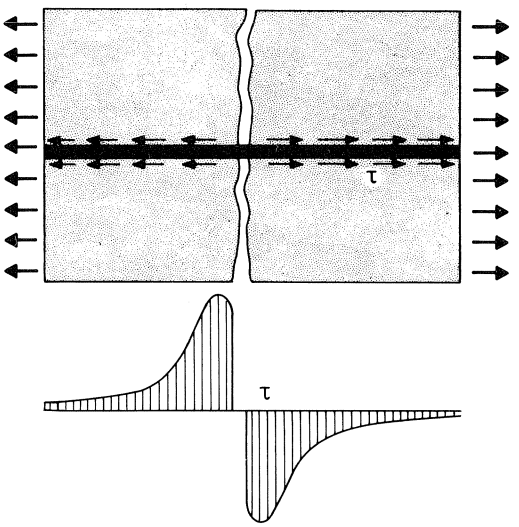

Fig. 3.5. Abrupt change of sign for the bond shear stress near a crack.

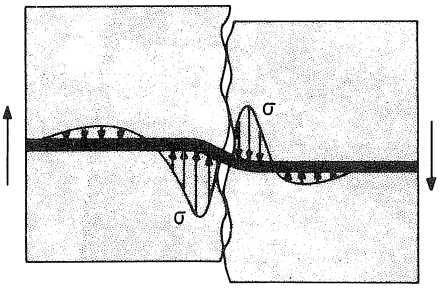

Fig. 3.6. Normal stresses between the bar and the concrete due to dowel action.

In this situation the boundary layer for bond is not in a state of axial symmetry, because the radial stress σ occurs only on one side of the bar. Such situations will occur more often, which means that in fact two separate bond layers are needed, one on each side of the bar.

3.2 *Analytical modelling*

The phenomena elaborated in Section 3.1 have to be modelled to allow for an analysis. We will hereafter show how this is done. In this section it will be explained which stress fields and displacement fields are applied. The constitutive relations between the stresses and the corresponding strains will be described in the next section. We start here with the situation of uncracked elements in Section 3.2.1 and will demonstrate in Section 3.2.2 what changes are to be made if cracks occur.

3.2.1 Uncracked state

Concrete element

In Chapter 2 it has been explained that a triangular element of a special type is used. We refer to this method as a hybrid method in which "natural boundary displacements" are used. In a standard type hybrid method according to Pian a distribution of stresses over the area of the element is chosen, and a separate independent interpolation is made for the displacements along the boundary of the element. The stress distribution satifies internal equilibrium conditions. The interpolation of the displacement is done using degrees of freedom at the corners of the elements. The two degrees of freedom at such a nodal point are common to all elements which meet at that node. So interelement compatibility is satisfied at forehand, but in general the interelement equilibrium of stresses is not achieved.

This standard type of hybrid elements was so modified that displacements are interpolated at the boundary for each element edge using separate degrees of freedom for each edge (natural boundary displacements), see Fig. 3.7. In this way the interelement equilibrium for the stresses along the element boundaries can be greatly improved.

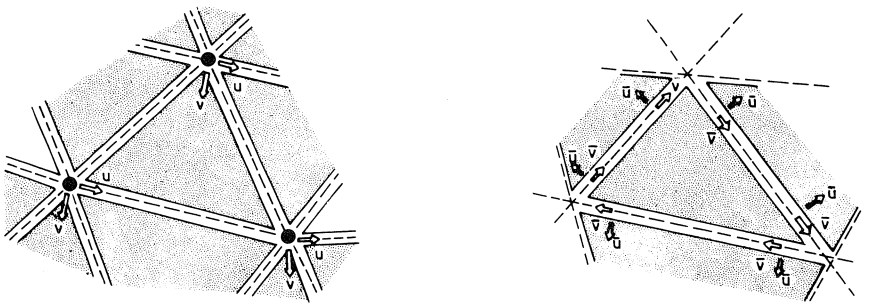

Fig. 3.7. Standard type of hybrid elements (left) and hybrid elements with natural boundary displacements (right).

This approach is considered to be of advantage for two reasons:

- the stress distribution in the elements can be chosen rather freely, which offers good possibilities for elements after cracking; the same applies to the displacements at the boundary;
- the favourable experience previously gained at Rijkswaterstaat could be used.

The four stresses σ_{xx}, σ_{yy}, σ_{xy} and σ_{yx} are linearly distributed over the element area; so they have different values at the three corners of an element. The interpolation is written in a bridged form as follows:

$$\sigma_{(x,y)} = P_1(x,y)\beta_1$$

in which $\sigma(x,y)$ is the vector of the stresses, β_1 is a vector of twelve stress parameters and $P_1(x,y)$ a matrix, whose coefficients are functions of x and y.

The displacements along one element edge are linearly interpolated. So, for two displacement components (one parallel to the edge and one normal to the edge), we need four degrees of freedom. In abridged form:

$$u(s) = L(s)v$$

in which $u(s)$ is a vector of two displacement components, v a vector of four degrees of freedom and $L(s)$ a matrix of two rows and four columns whose terms are linear functions of the coordinate s, which is chosen along the edge in consideration.

The distributions for $\sigma(x,y)$ and for $u(s)$ cannot be chosen completely freely. In the hybrid theory some rules have to be obeyed which relate the distributions to each other. These conditions are fully dealt with in [4].

The element results in a stress distribution which satisfies the conditions of equilibrium within the area of the element (Fig. 3.6).

$$\sigma_{xx,x} + \sigma_{xy,y} = q_x$$
$$\sigma_{yx,x} + \sigma_{yy,y} = q_y$$

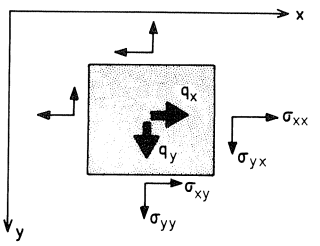

Fig. 3.8. Equilibrium conditions.

Note that the stresses σ_{yx} and σ_{xy} in this report do not correspond to the convention of the index notation. These stresses do not satisfy the condition that σ_{xy} is equal to σ_{yx} at each each point (x,y) of the element, but satisfy this condition only in an average sense

$$\int_{A_e}\int (\sigma_{xy} - \sigma_{yx})\, \mathrm{d}A = 0$$

in which A_e is the area of the element. This approach was necessary to meet the conditions of the hybrid method referred to earlier. It means that the element incorporates some characteristics of the Reissner-Hellinger principle.

Reinforcing bar element

We shall now consider the connection of an uncracked triangular element and a reinforcing bar (Fig. 3.9).

The concrete elements each transmit a linear distribution of normal stresses σ and tangential stresses τ to a reinforcement element. The linear stress τ causes a quadratic distribution of the normal force F in the bar. This implies that the two element forces at the end of an element need not be equal to each other. These two forces correspond to two axial degrees of freedom. The linear stress σ causes a quadratic shear force S in the bar and a cubic distribution for the bending moments M in the bar element. In general the described distribution for the shear force S and the bending moment M result in two element forces at each end of a bar element, a force acting normal to the bar axis and a moment. This implies that at each end two corresponding degrees of freedom are necessary, a displacement normal to the bar axis and a rotation. The author of the program has decided to omit the rotation of a bar element end and included only two displacements, one axial and one normal to the bar axis. So the bar elements are connected by hinges to each other. This choice makes the bending moments zero at the ends of the bar and ensures that the bending moments in the bar remain small. The average shear force in an element will always be zero. Furthermore it was decided not to take account of the bending stiffness of the bar element but only to consider the shear rigidity (the "dowel" rigidity along the length of a bar element). So, for the bar element the normal force F and the shear force S, and their corresponding strains ε and γ, are of importance. The stiffness relations are:

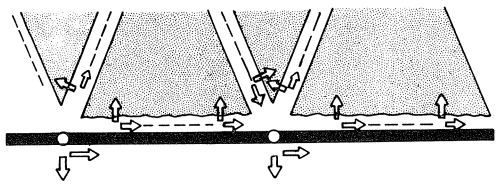

Fig. 3.9. Chosen connection of reinforcement to concrete.

$$\begin{bmatrix} \varepsilon \\ \gamma \end{bmatrix} = \begin{bmatrix} \frac{1}{AE} & 0 \\ 0 & \frac{1}{D} \end{bmatrix} \begin{bmatrix} F \\ S \end{bmatrix}$$

where

ε = strain of steel
γ = deformation in steel due to shear force
A = cross-sectional area of steel
E = modulus of elasticity of steel
D = "dowel" rigidity of steel

Bond zone element

The boundary layer for bond between the reinforcing bar element and the concrete element can easily be added to the model. As shown in Section 3.1, this layer is represented by a stiffness relation between the stresses τ and σ acting on it and the corresponding deformations $\Delta_{//}$ and $\Delta_{\perp}$. The stresses are related to the forces in the bar element according to

$$\tau = \frac{dF}{ds}$$

$$\sigma = \frac{dS}{ds}$$

The stiffness relation is adopted as:

$$\begin{bmatrix} \Delta_{//} \\ \Delta_{\perp} \end{bmatrix} = \begin{bmatrix} \frac{1}{K} & 0 \\ 0 & \frac{1}{B} \end{bmatrix} \begin{bmatrix} \tau \\ \sigma \end{bmatrix}$$

where

$\Delta_{//}$ = parallel displacement in boundary layer
$\Delta_{\perp}$ = widening of boundary layer
K = rigidity of boundary layer with respect to a parallel displacement
B = rigidity of boundary layer with respect to the widening

The stiffness relation adopted is considered to be a preliminary one. The final results of the "Betonmechanica" project 2, which is studying the bond zone in more detail, are awaited. The diagonal rigidity matrix chosen here may then be replaced by a fully filled matrix.

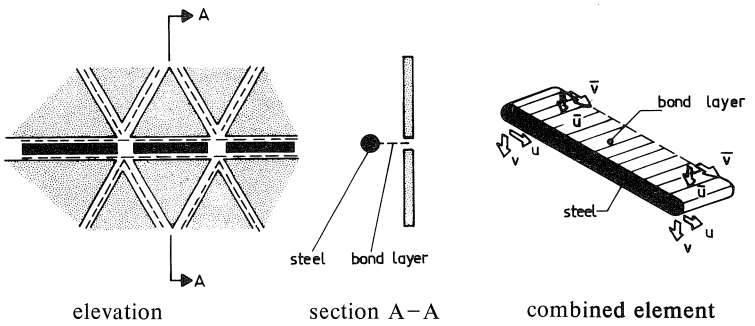

Fig. 3.10. Connection of steel bar and bond layer to the concrete elements in the present-day version of MICRO/1.

As has been described here, the bar element and the boundary layer element are separate elements. In the implementation in the program they were assembled to one combined element. No distinction is made in the present version of the program between the two different bond layers on each side of a bar element. The overall behaviour is comprised on one bar-boundary-layer element. Fig. 3.10 shows how the connection between the combined bar element and the concrete elements should be conceived. It implies that the two concrete elements on both sides of a bar element will have the same displacements at this position.

3.2.2 Cracked state

If the stresses in a plate element attain the magnitudes at which (according to the cracking criterion) the concrete cracks, a discrete crack is assumed to form, extending in a straight line from one boundary of the element to another. Not more than two cracks per plate element are permitted. For these cracks the limiting condition imposed is that they must intersect each other at an element boundary and that they must, from this point of intersection, each extend to a different side of the triangle. This requirement results from the rule applied, namely, that at each side of the triangle only one point of intersection with a crack is allowed to occur (Fig. 3.11).

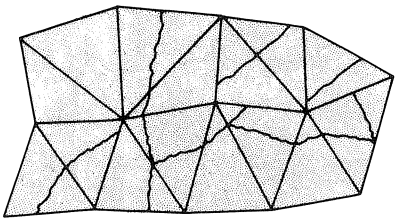

Fig. 3.11. Possible cracks in the triangular elements.

The crack direction is assumed to be perpendicular to the principal tensile stress. The position of a crack within a triangular element is so determined that the crack links up with a crack already present in an adjacent element. If the boundaries of the element under consideration have not yet been encountered by a crack in adjacent elements, the crack is assumed to pass through the centre of gravity of the triangle.

In a cracked element the three possible ways in which the parts thereof can undergo displacement as a rigid body are taken into account. To this end, the following displacements are considered at a crack:

- the displacement of the two crack faces relatively to each other perpendicularly to the direction of the crack,
- the displacement of the two crack faces relatively to each other in the direction of the crack,
- the rotation of the two crack faces relatively to each other.

The result of this is a linear distribution of the crack widening along the crack and a constant shift along the crack. Therefore within a crack three additional degrees of freedom are introduced. Two of them (u_i and u_j) describe a linearly varying crack opening, and one (v) is used to describe the parallel shift (Fig. 3.12). The natural boundary displacements $\bar{u}$ and $\bar{v}$ at the outer edges have to be adjusted if a crack crosses an edge.

This is done by adding a discontinuous displacement interpolation to the linear displacement interpolation of an uncracked element. This implies the additional degrees of freedom Δu^0 and Δv^0, shown in Fig. 3.12.

In the vicinity of a crack the stresses may vary greatly due to dowel forces in the bars or to bond stresses between the bars and the concrete. To take account of these stress variations and of the possibility of the normal stress at a crack displaying a discontinuity in the crack direction, the linear stress field of the uncracked element is extended, for a cracked element, by a stress field which is discontinuous across the crack, to:

$$\sigma(x,y) = P_1(x,y)\beta_1 + P_2(x,y)\beta_2$$

The discontinuous part of the additional stress field $P_2(x, y)\beta_2$ is shown in Fig. 3.13 (the distribution along the element edges).

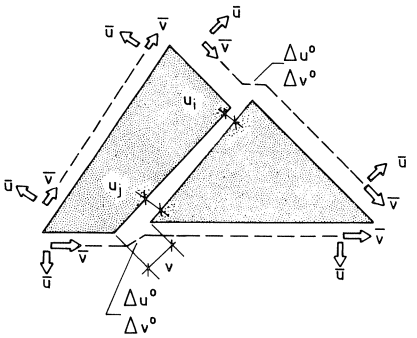

Fig. 3.12. Additional displacements u_i, u_j and v in the crack, and Δu^0 and Δv^0 for the discontinuous displacement interpolation at the element boundary.

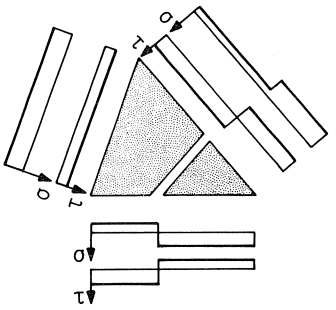

Fig. 3.13.
Distribution of the stresses, according to the discontinuous part of the additional stress field, along the boundaries of a plate element with one crack.

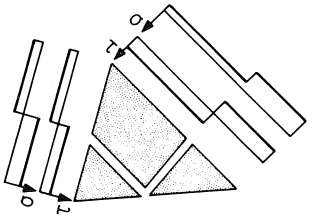

Fig. 3.14.
Distribution of the stresses, according to the discontinuous part of the additional stress field, along the boundaries of a plate element with two cracks.

The choice of this stress field and the corresponding displacements Δu^0 and Δv^0 preserves full inter-element equilibrium in a element boundary crossed by a crack.

In an element a second crack is permitted only if this crack runs from the uncracked edge to the intersection of the first crack and the element boundary (see Fig. 3.14). Now the additional stress field is discontinuous over both cracks and we find additional degrees of freedom along all three element boundaries.

If a *bar element* is intersected by a crack, then – as in the plate element – the stress functions and displacement functions are extended by adding extra fields. These fields are compatible with the extra stresses and displacements used in the plate element. The constant additional fields for τ and σ yield linear additional fields for the normal force F and the shear force S (Fig. 3.15).

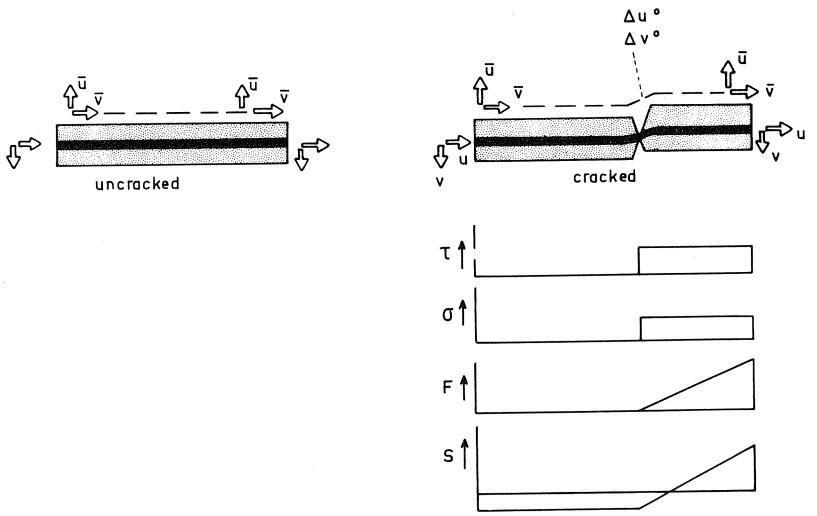

Fig. 3.15. Extra stress fields and degrees of freedom in a bar element intersected by a crack.

On briefly assessing the choices made for the cracked state, the following can be stated. The analytical model fully allows for aggregate interlock and bond. It will depend on the mesh fineness whether or not the bond stresses near a crack can be dealt with correctly (see Fig. 3.5). The abrupt change can be described, but we shall need a number of elements to follow the rapidly damping nature of the local phenomenon. It is more doubtful if the dowel action (see Fig. 3.6) is modelled correctly. Here we shall also need a couple of elements to describe the rapidly varying local phenomenon; it may be a shortcoming of the analysis that as yet no bending of the steel bar is considered.

3.3 *Material properties*

Section 3.2 defined what stresses and related deformations occur in the analytical model. In this section we shall describe which constitutive laws are used to relate the stresses to the deformations. The behaviour of a material is always described with the aid of a number of models, each of which describes a particular aspect of the behaviour. In the Preface these models are called the *basic* or material models, in order to distinguish them from the overall models for the analysis of a structure, such as the Micro-model, in which the basic models are used. The latest knowledge concerning the behaviour of the materials is embodied in the basic models. More particularly with regard to concrete, however, the available knowledge of its behaviour under various conditions is still very incomplete, and research on the subject is still in full swing. The Micro-model has therefore been conceived such that the basic models can quite simply be replaced by others or be increased in number.

The Micro-model comprises basic models for the following material properties for concrete:
- a non-linear stress-strain relationship,
- a cracking criterion for concrete in tension,
- a crushing criterion for concrete in compression,
- a shrinkage model,
- a creep model,
- a model for aggregate interlock in a crack;

for steel:
- a non-linear stress-strain relationship;

for the boundary layer between steel and concrete:
- a non-linear shear stress-displacement relationship,
- a non-linear normal stress displacement relationship.

For some material properties alternative models have been included, from which the user can make a choice according to his own judgement. No experimental research into the behaviour of the materials has been undertaken within the context of this study. With the exception of the model for aggregate interlock in a crack, the basic models for the description of the concrete properties have been taken from the literature. Where several models are reported in the literature, a choice has been made on the basis of agreement with experiments and of the serviceability of such models in the Micro-

model. Pending the results of research on the force-displacement relations in a crack and on the cooperation between steel and concrete, which is being carried out within the framework of the "Betonmechanica" project (see Preface), simple linear elastic and elasto-plastic models for the properties have been adopted. No models have been included for describing the relaxation of prestressing steel and the time-dependent deformations at a crack and in the boundary layer. The reason for not (yet) taking account of the two last-mentioned creep deformations is the existing lack of knowledge concerning these deformations. In comparison with the creep of concrete, the relaxation of steel is such a rapid process that it is assumed to have been completely accomplished before the concrete starts its creep.

3.3.1 Constitutive laws for concrete

The MICRO/1 program can be used with two alternative basic models for plane concrete, one due to Link and one due to Buyukozturk. Both will be described and if modifications were made, they will be indicated.

3.3.1.1 Link's model

This model comprises a non-linear stress-strain relationship, a criterion for cracking and a crushing criterion for concrete in compression. These two criteria are *stress* criteria [7].

Non-linear stress-strain relation

This model is based on results of experimental research by Kupfer et al. concerning the behaviour of concrete under two-dimensional states of stress. Basing himself on these results, Link developed formulas for the calculation of the strains (ε) associated with any (arbitrary) two-dimensional state of stress. These formulas define the total strains depending on the actual stresses, the uniaxial compressive strength of concrete, the initial modulus of stiffness and the initial value of Poisson's ratio. Presupposing coincidence of the orientation of the principal directions of the stress tensor and the strain tensor, and assuming symmetry of the stress-strain relationship, Link formulates the constitutive relationship as follows:

$$\begin{bmatrix} \varepsilon_{11} \\ \varepsilon_{22} \end{bmatrix} = \begin{bmatrix} \frac{1}{E_1^s} & -\frac{\nu_1^s}{E_1^s} \\ -\frac{\nu_2^s}{E_2^s} & \frac{1}{E_2^s} \end{bmatrix} \begin{bmatrix} \sigma_{11} \\ \sigma_{22} \end{bmatrix}$$

The symbols in the relationship have the following meanings:

E_i^s = secant modulus of elasticity in the principal direction i
ν_i^s = secant value of Poisson's ratio in the principal direction i
σ_{ii} = principal stress in the direction i
ε_{ii} = principal strain in the direction i

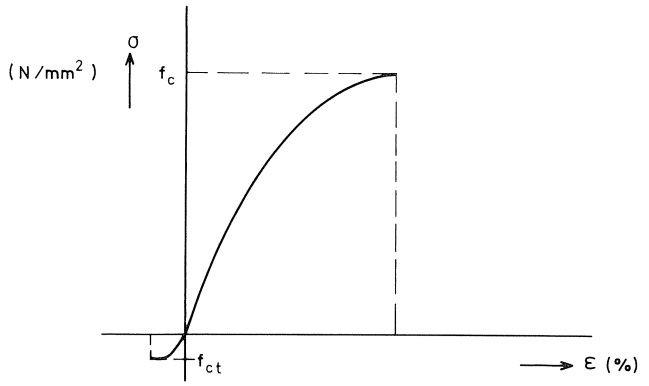

Fig. 3.16. Stress-strain for uniaxial state of stress for Link's model.

For the very elaborate formulas for E_i^s and v_i^s the reader is referred to [7].

To give an impression of the nature of those formulas, the result is sketched for a uniaxial state of stress in Fig. 3.16. This is indeed the type of stress-strain diagrams found by Kupfer et al. in their experimental investigations. Link obtained his formulas through curve fitting of these results.

The model is in good agreement with the experimental results of various investigators. Besides this advantage, it has some disadvantages, however, namely:

- the model is purely elastic and therefore takes no account of the permanent deformations that remain on unloading, nor of the dependence of the strains upon the stress path followed,
- the assumptions made in deriving the formulas have yet to be investigated as to their validity,
- the elaboration and precision of the formulas suggests an accuracy which is decidedly unrealistic with reference to a material such as concrete.

Cracking criterion

In considering the behaviour of concrete subjected to two-dimensional states of stress a distinction is drawn between the crushing and the cracking of the concrete.

By cracking is here understood the formation of cracks in the concrete perpendicularly to the plane of the two-dimensional state of stress. These cracks develop if one of the principal stresses is positive (tensile stress) or if both of them are positive. Many authors make use of a *stress* envelope as shown in Fig. 3.17 for describing the states of stress for which these cracks arise. This general approach is also adopted by the author of the MICRO/1 program.

The values *SB*, *SA* and $\tan(\alpha)$ are needed for describing this criterion. The points *A* mark the transition from the cracking criterion to the region where crushing of the concrete occurs. Experimental results indicate for $\tan(\alpha)$ values ranging from $\frac{1}{10}$ to $\frac{1}{15}$.

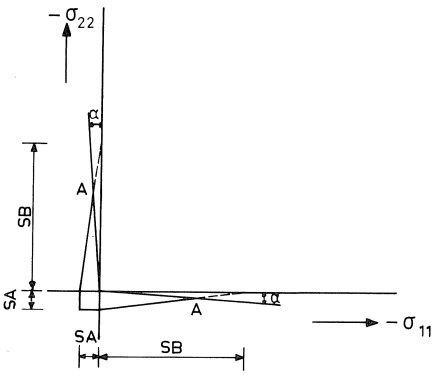

Fig. 3.17. Criterion of cracking

For the calculations performed for this report the following have been adopted:

$S_A = f_{ct}$ = uniaxial tensile strength of concrete
$S_B = f_{cc}$ = uniaxial compressive strength of concrete
$\tan(\alpha) = \frac{1}{15}$

It is assumed that if the stresses attain a value located on this cracking stress envelope, a crack is formed perpendicular to the larger principal stress (= tensile stress) and the stresses at right angles to this crack have to become zero.

Crushing criterion

By crushing of concrete is understood the formation of cracks both in, and perpendicular, to the plane of the two-dimensional state of stress. This type of cracking occurs if one or both of the principal stresses are approximately equal to the monoaxial compressive strength of concrete. As a result of such cracking the ability of the concrete to transmit large compressive stresses is reduced. In Link's constitutive model of concrete no account has been taken of the post-crushing strength. It has not been attempted to extend the model for this aspect. In stead, a fictitious slightly inclined branch has been added to achieve that the numerical iteration process will come to a good result.

The model for the failure criterion of concrete according to Link [7] is, like his constitutive model, based on the tests of Kupfer et al. His original criterion is valid both for failure in cracking and for failure in crushing. In the Micro-model this model according to Link is used only to describe the crushing of concrete. The transition from cracking criterion to crushing criterion is located at the points A for which the value of $\tan(\alpha)$ is equal to $\frac{1}{15}$. Using the method of "curve fitting", Link has established a number of formulas for the failure envelope for various kinds of concrete. He even suggests a generally-applicable formula for normal weight concrete. The shape of this function is shown in Fig. 3.18. This formula is also used in MICRO/1.

The model is in good agreement with the experimental results of Kupfer et al. However, this model likewise has the drawback of taking no account of the stress history and of giving an exaggerated impression of accuracy. Moreover, the model does not provide a facility for softening after crushing has occurred.

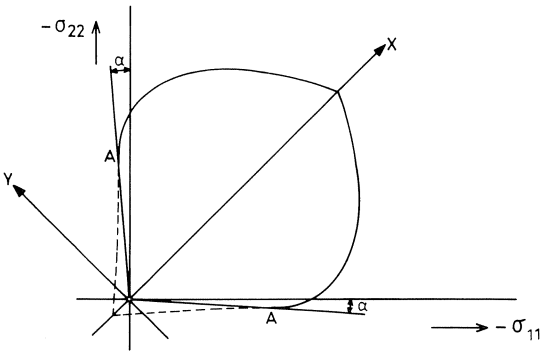

Fig. 3.18. Link's crushing envelope.

3.3.1.2 Buyukozturk's model

Link's model may prove inadequate for analysing the behaviour of structures which, after being loaded, are unloaded or on which the various loads are not simultaneously increased monotonically. A constitutive model for concrete which does take account of permanent deformations and also of the dependence of the strains upon the "stress history" is that of Buyukozturk [8]. His work is also based on the experimental investigations of Kupfer et al., so no major differences can occur with Link's model. The main distinction is that this model is based on the conception of elasto-plastic material behaviour supplemented with isotropic strain hardening in consequence of plastic deformations. The main aspects of the model are demonstrated in Fig. 3.19.

In the plane of principle stresses σ_{11} and σ_{22} two surfaces are indicated. The inner one is the yield surface. For stress states which remain inside this surface the concrete behaves in a linearly elastic manner.

On crossing this surface the concrete starts yielding, but because of isotropic hardening the stresses can still increase as wel as the strains, which then consist of an elastic

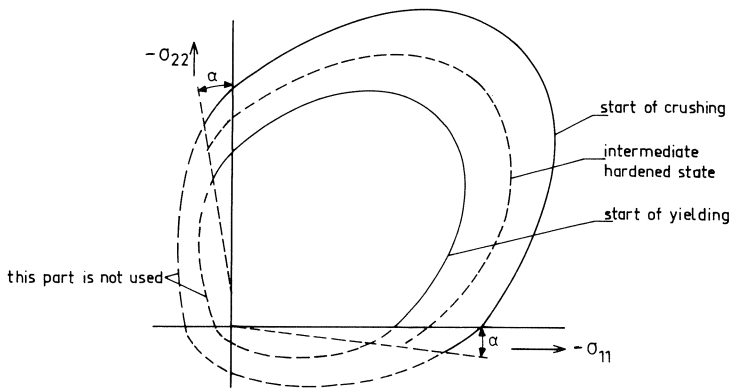

Fig. 3.19. Plot of the yield criterion and crushing criterion in the Buyukozturk's model.

part ε and a plastic part ε^p. For general states of strain an equivalent plastic strain $\bar{\varepsilon}^p$ has to be defined to measure the amount of plastic deformation. Similarly, an equivalent stress $\bar{\sigma}$ has to be introduced which defines the position of a yield envelope. This equivalent stress increases for increasing equivalent strain, causing the envelope to move outwards. It is necessary to adopt a strain hardening rule $\bar{\sigma} = H(\bar{\varepsilon}^p)$ to relate $\bar{\sigma}$ and $\bar{\varepsilon}^p$ to each other. When the equivalent strain reaches a critical maximum value $\bar{\varepsilon}^p_{\max}$, the concrete starts crushing. This is the case for states located on the outer envelope in Fig. 3.19. Outside this crushing surface combinations of stress σ_{11} and σ_{22} can still occur, because the concrete still can transmit some stress. Buyukozturk did not include a post-crushing branch in his model. The author of MICRO/1 has assumed that on attainment of the crushing criterion there occurs a transition from an isotropic hardening model to an isotropic softening model. In a uniaxial state of stress the modified model of Buyukozturk is thus represented by Fig. 3.20. The value of the stress, α_0 at the end of the elastic region is about one-third of the concrete crushing strength in compression f_c.

We see in the diagram (as was the case in Link's model) a cut-off in the branch for tensile stress, due to cracking. Buyukozturk himself did not formulate a cracking criterion. He only defined a failure criterion for cases where both principal stresses are negative (compression). For the compressive/tensile and the tensile/tensile region he adopts the cracking criterion which is also used in conbination with the Link model. As applied by Buyukozturk, the crack criterion and the crushing criterion are both *stress* criteria.

The author of MICRO/1 has slightly modified Buyukozturk's overall concept for the failure criterion (both cracking and crushing). He considers the transition from crushing with cracks to occur at a value of -15 and $-\frac{1}{15}$, respectively, for the ratio σ_{11}/σ_{12} (or, stated differently: $\tan(\alpha) = \frac{1}{15}$). So it is assumed that the crushing criterion for the case where both principal stresses are negative (compression) also holds for a part of the compressive/tensile region (see full lines in Fig. 3.19). In the approach of MICRO/1 the crushing criterion is considered to be a *strain* criterion. It corresponds to a maximum value for the equivalent plastic strain ($\bar{\varepsilon}^p_{\max}$). Having now given a "helicopter" view of the modified Buyukozturk model, we shall describe in more detail the linear stress-strain

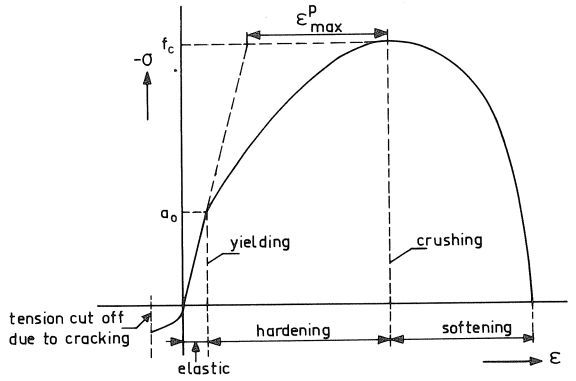

Fig. 3.20. Stress-strain diagram for uniaxial state of stress for the modified Buyukozturk's model.

relation, the cracking criterion and the crushing criterion, and give an account of the hardening and softening model.

Linear stress-strain relation

In the elastic region of the stress space the constitutive relation for the Buyukozturk model is:

$$\begin{bmatrix} \varepsilon_{11} \\ \\ \varepsilon_{12} \end{bmatrix} = \frac{1}{E} \begin{bmatrix} 1 & -\nu \\ \\ -\nu & 1 \end{bmatrix} \begin{bmatrix} \sigma_{11} \\ \\ \sigma_{22} \end{bmatrix}$$

where

ε_{ii} = principal strain in direction i
σ_{ii} = principal stress in direction i
E = modulus of elasticity
ν = Poisson's ratio

Cracking criterion

See the explanation for the Link model and Fig. 3.17. The same applies to the Buyukozturk model.

Yield and crushing criterion, equivalent stress

Buyukozturk uses a "generalized Mohr-Coulomb" formula for the yield surface F:

$$F = 3\sqrt{3J_2 + \bar{\sigma} J_1 + \tfrac{1}{5} J_1^2} - \bar{\sigma} = 0$$

For two-dimensional states of stress the symbols in this formula denote

$J_1 = \sigma_{xx} + \sigma_{yy}$
$J_2 = \tfrac{1}{3}(\sigma_{xx}^2 + \sigma_{yy}^2 - \sigma_{xx}\sigma_{yy}) + \tfrac{1}{4}(\sigma_{xy} + \sigma_{yx})^2$
$\bar{\sigma}$ = equivalent stress

When yielding starts, the equivalent stress $\bar{\sigma}$ has the value α_0 (see Fig. 3.20), which is about one-third of f_c; $\bar{\sigma}$ increases for growing values of the plastic strains up to the maximum value f_c when crushing occurs. Thereafter it decreases for increasing values of plastic strains until it becomes zero. The concrete has then become totally exhausted.

Strain hardening rule; equivalent strain

When yield occurs, plastic strains will develop. According to the Prandtl-Reuss assumption, with isotropic hardening the plastic strain increments $\mathrm{d}\varepsilon^p$ are perpendicular to the surface F. We can write this as follows:

$$\mathrm{d}\varepsilon^p = \mathrm{d}\bar{\varepsilon}^p \left\{\frac{\partial F}{\partial \sigma}\right\}$$

where $d\bar{\varepsilon}^p$ is the increase of the equivalent plastic strain and $\{\partial F/\partial\sigma\}$ denotes the vector which defines the direction of the plastic strain increment. Note that $d\bar{\varepsilon}^p$ is zero if $F \leqslant 0$ and that it is positive unequal non-zero if $F > 0$.

In the MICRO/1 program the increase of the equivalent strain ($d\bar{\varepsilon}^p$) per loading stage is defined as (using index notation and summation convention).

$$d\bar{\varepsilon}^p = \sqrt{\tfrac{2}{3}\, d\varepsilon_{ij}^p\, d\varepsilon_{ij}^p}$$

This is a normal convention in elasto-plastic models.

How to sum the contributions $d\bar{\varepsilon}^p$ of all n stages of analysis presents a problem, for a strain path in the strain space need not be in the same direction at each stage. Indications exist that plastic deformations in the case of biaxial compressive loading are about 20% less than in the case of monoaxial compressive loading. This means in fact that we have to use different strain hardening rules $\bar{\sigma} = H(\bar{\varepsilon}^p)$, depending of the state of stress. This is, however, not practicable. In the MICRO/1 program the strain hardening rule for mono-axial loading is used for all states of stress, but the equivalent strain $\bar{\varepsilon}^p$ is adjusted artificially in each stage of analysis to account for the differences in hardening. To decide how to do this we have to bear in mind that we want to predict the new value of the equivalent stress $\bar{\sigma}$ after an increase in $\bar{\varepsilon}^p$. Given a magnitude $\bar{\varepsilon}^p$ in biaxial loading, we can use the strain hardening rule for mono-axial loading to find the appropriate new value of $\bar{\sigma}$ by taking a greater value of $\bar{\varepsilon}^p$. In the MICRO/1 program this increase is chosen to be 20%. In other words, the equivalent strain $\bar{\varepsilon}^p$ is weighed with a multiplication factor α of the value 1,2.

This procedure has also been used in the compressive/tensile region of the stress space in order to achieve a smooth transition from the compressive region to the tensile region. Surveying all possible states here from mono-axial compression up to mono-axial tension, it can be presumed that the occurrence of plastic strains will strongly decrease. Yet the strain hardening rule for mono-axial compression in this whole region can still be used by again introducing the factor α, which now ranges from the value 1 up to a high value, for which the value 10 is chosen.

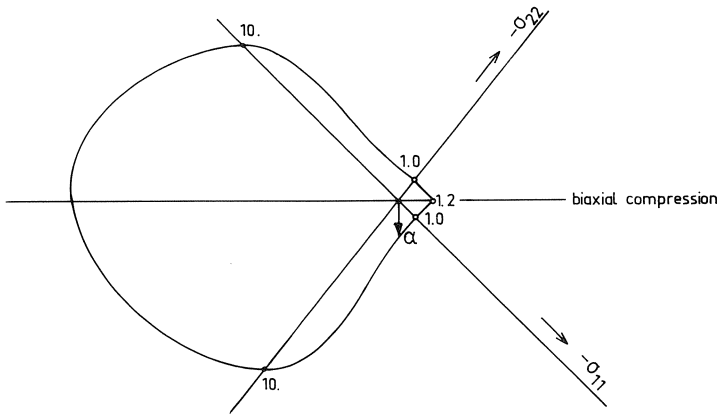

Fig. 3.21. Weighing factor α for adjusting the equivalent plastic strains.

Fig. 3.21 shows a plot for the chosen values of α in the two-dimensional stress space. It is described by the following formula:

$$\alpha = \frac{\bar{\sigma}}{\sqrt{\sigma_{11}^2 + \sigma_{22}^2 - \frac{3}{2}\sigma_{11}\sigma_{22}}}$$

This formula is also applied in the tensile/tensile region. It causes artificial intensive hardening there, which implies rapid growth of the stress. So the crack criterion will become dominant very soon. Summing up, we can calculate an (artificial) total plastic strain $\bar{\varepsilon}^p$ as follows:

$$\bar{\varepsilon}^p = \sum_{i=1}^{n} \alpha_i \, \mathrm{d}\bar{\varepsilon}_i^p$$

This total plastic strain is used in the relationship between $\bar{\sigma}$ and $\bar{\varepsilon}^p$ for mono-axial loading in compression. In MICRO/1 a second order polynomial is used for this relationship:

$$\bar{\sigma} = \alpha_0 + \alpha_1 \bar{\varepsilon}^p + \alpha_2 (\bar{\varepsilon}^p)^2$$

The coefficients α_0, α_1 and α_2 are to be so calculated that $\bar{\sigma}$ is about one-third of the crushing strength f_c for zero value of $\bar{\varepsilon}^p$ and that $\bar{\sigma}$ equals f_c when $\bar{\varepsilon}^p$ reaches the maximum value $\bar{\varepsilon}^p_{\max}$. For this value of the strain the derivative $\mathrm{d}\bar{\sigma}/\mathrm{d}\bar{\varepsilon}^p$ must be zero.

It is not easy to specify an isotropic softening model for concrete for values of $\bar{\varepsilon}^p$ larger than $\bar{\varepsilon}^p_{\max}$, no experimental results being available. In MICRO/1 is has been assumed that the second order polynomial for $\bar{\sigma}$ also holds for softening. We then get the curve plotted in Fig. 3.20.

It must once again be pointed out that the validity of the various assumptions adopted in the analysis has not yet been sufficiently verified by experimental results. From the limited amount of comparative information available it does, however, already emerge that the supposed orthogonality of the increase of the plastic strains and the yielding surface may not be correct.

3.3.2 Shrinkage of concrete

The shrinkage deformation of concrete is here considered independently of the state of stress and of the creep deformation. Recent research shows that there is indeed a connection between shrinkage and creep. These investigations had, however, at the start of the MICRO/1 program not yet resulted in a model that can be incorporated into an overall model. The model for shrinkage employed here is based on CEB Report 111 (1975) [9].

The shrinkage deformation is determined with the formula:

$$\varepsilon(j) = \sum_{i=1}^{j} \varepsilon_b \{R(i)\} * [K_s(F_{dk'} t_{c1}\{i+1\}) - K_s(F_{dk'} t_{c1}\{i\})]$$

where:

$\varepsilon(j)$ = shrinkage strain after the j^{th} day
$\varepsilon_b\{R(i)\}$ = basic shrinkage (final shrinkage value)
F_{dk} = corrected fictitious thickness
$t_{c1}^{(i)}$ = corrected age
$K_s(F_{dk}, t_{c1})$ = function describing shrinkage behaviour
$R(i)$ = relative humidity at day i
j and i = time in days

The corrected fictitious thickness is

$$F_{dk} = k_w * \text{actual thickness}$$

The factor k_w is dependent on the humidity of the environment. The basic shrinkage ε_b is dependent on the degree of drying of the concrete, which in turn depends to a great extent on the relative humidity of the environment of the structure. No tables or formulas for the basic shrinkage are included in the program. This shrinkage has to be stated for each period of time by the user of the program. The function K_s with which shrinkage behaviour is described is dependent on the corrected fictitious thickness F_{dk} and the corrected age t_{c1}. The program comprises tables for determining K_s; these tables are based on the graphs published in [9] (see Fig. 3.22).

The corrected age is determined with the formulas:

$$t_{c1}^{(j)} = \sum_{i=1}^{j} \frac{T(i) + 10°}{30°} \Delta t_i$$

where $T(i)$ is the temperature in degrees centigrade on day i.

For each period of time the following quantities have to be introduced into the program:
- the basic shrinkage ε_b
- the temperature T
- the end time of the period j
- the correction factor for the thickness k_w

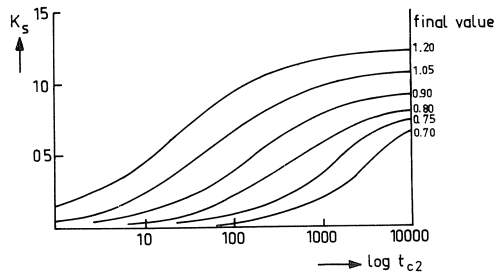

Fig. 3.22. Function K_s.

3.3.3 Creep of concrete

Like the model for shrinkage, the model for creep is based on CEB Report 111 (1975). Creep deformation is determined by applying a multiplying factor φ to the non-time-dependent non-linear deformation. By basing the calculation of creep deformation on the total non-time-dependent deformation it is ensured that at high compressive stresses (> 0.5 compressive strength) the creep deformation is no longer proportional to the stress, but increases progressively.

The creep model comprises two parts;
- the recoverable creep, sometimes referred to as the delayed elastic deformation,
- the irrecoverable creep.

The creep deformation after day j is determined with the formula

$$\varepsilon_{creep}(j) = \sum_{i=1}^{j} \varepsilon^*(i)[\varphi_p * (K_p\{F_{dk}, t_{c2}(i+1)\} - K_p\{F_{dk}, t_{c2}(i)\}) +$$

$$\varphi_r * (K_r\{t_{c2}(i+1) - t_{c2}(i)\}) * (1 - K_r\{t_{c2}(j+1) - t_{c2}(i+1)\})]$$

where:

$\varepsilon_{creep}(j)$	= vector with creep strains after day j
$\varepsilon^*(i)$	= vector with non-time-dependent non-linear strains at day i
φ_p	= final value of irrecoverable creep deformation
φ_r	= final value of recoverable creep deformation
$K_p(F_{dk}, t_{c2})$	= function describing irrecoverable creep behaviour
$K_r(t_{c2})$	= function describing recoverable creep behaviour
F_{dk}	= corrected fictitious thickness
$t_{c2}(j)$	= corrected age

The quantities φ_p and F_{dk} are dependent on the relative humidity of the environment of the structure. As in the case of shrinkage, no tables or formulas for the values φ_p and φ_r have been included in the program. The program user has to state these quantities for each period of time. The corrected fictitious thickness is calculated with the formula:

$$F_{dk} = k_w * \text{actual thickness}$$

The factor k_w is dependent on the humidity of the environment. The corrected age t_{c2} is dependent on the temperature and on the type of cement. The following formula has been adopted for determining t_{c2}:

$$t_{c2}(j) = k_z \sum_{i=1}^{j} \frac{T(i) + 10°}{30°} \Delta t_i$$

where $T(i)$ is the temperature in degrees centrigrade on day i and k_z is a factor depending on the type of cement employed.

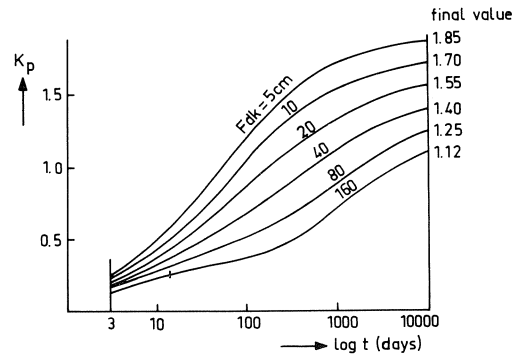

Fig. 3.23. Function K_p.

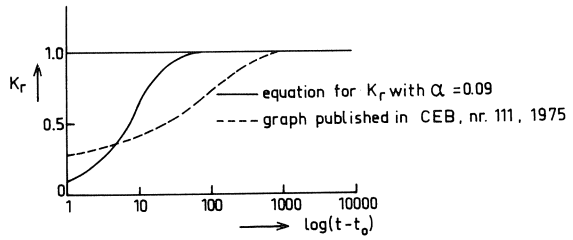

Fig. 3.24. Function K_r.

The graphs for K_p (Fig. 3.23) are incorporated in the form of a table in the program. The graph (Fig. 3.24) representing the behaviour of K_r has been converted into the formula:

$$K_r = \{1 - e^{-\alpha(t_{c2} - t_0)}\}$$

The numerical value of the factor α can be stated by the user; $\alpha = 0.09$ is recommended.

By describing the recoverable creep with the aid of a Kelvin element this creep can, per period of time, be completely determined from the stresses and the recoverable creep that has already occurred at the beginning of the period. Hence it is not necessary to remember the whole stress history. The increase in creep deformation thus becomes:

$$\varepsilon_{\text{creep}}(j+1) - \varepsilon_{\text{creep}}(j) = \Delta\varepsilon_{\text{creep}}(j+1) = \varepsilon^*(j+1)[\varphi_p^*(K_p\{F_{dk}, t_{c2}(j+2)\} +$$

$$- K_p\{F_{dk}, t_{c2}(j+1)\})] + \sum_{i=1}^{j+1} \varepsilon^*(i)[\varphi_r^*(1 - e^{-\alpha t_{c2}(i+1)} * e^{\alpha t_{c2}(i)}) *$$

$$(e^{-\alpha t_{c2}(j+2)} * e^{\alpha t_{c2}(i+1)})] - \sum_{i=1}^{j} \varepsilon^*(i)[\varphi_r^* e^{-\alpha t_{c2}(j+1)} * (e^{\alpha t_{c2}(i+1)} - e^{\alpha t_{c2}(i)})]$$

Hence:

$$\Delta\varepsilon_{\text{creep}}(j+1) = \varepsilon^*(j+1)\varphi_p * \Delta K_p + \varepsilon^*(j+1)\varphi_r^*(1 - e^{-\alpha t_{c2}(j+2)} * e^{\alpha t_{c2}(j+1)}) *$$

$$\varepsilon_r(j) * (e^{-\alpha t_{c2}(j+2)} - e^{-\alpha t_{c2}(j+1)})$$

In this formula for the creep deformation increase the symbol $\varepsilon_r(j)$ denotes the recoverable creep deformation after the j^{th} day. For each period of time the following quantities have to be introduced into the program:

- the final value of the irrecoverable creep φ_p
- the final value of the recoverable creep φ_r
- the temperature T
- the correction factor for the thickness k_w
- the correction factor for fictitious time k_z

3.3.4 Aggregate interlock in a crack

The generalized aggregate interlock as defined in section 3.2 requires a relation between τ and σ, on the one hand, and $\Delta_{//}$ and $\Delta_{\perp}$, on the other hand. Because the results of the "Betonmechanica" project concerning force transfer in cracks were not available when writing the program MICRO/1, a preliminary assumption was made. Pending those results a rigid-plastic model was adopted for the parallel displacement $\Delta_{//}$ at a crack and the shear stress τ (Fig. 3.25).

The maximum shear stress (τ_{max}) that can be transmitted in a crack will depend on the crack width $\Delta_{\perp}$. The following relation is assumed:

$$\tau_{max} = \frac{1}{k\,\Delta_{\perp}}$$

where

$\Delta_{\perp}$ = crack width
k = constant

In Fig. 3.26 the variation of τ_{max} with $\Delta_{\perp}$ is shown.

In MICRO/1 it is assumed that no tensile stress can occur normal to a crack.

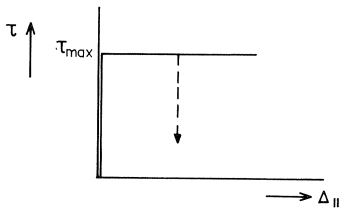

Fig. 3.25. Rigid-plastic model for aggregate interlock in a crack.

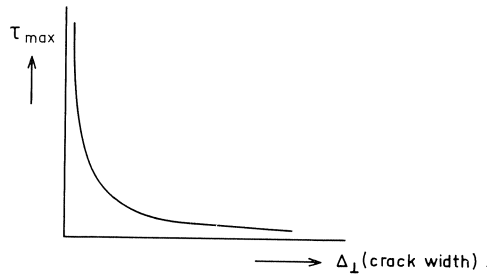

Fig. 3.26. Maximum shear stress as a function of crack width.

3.3.5 Behaviour of the steel

The program incorporates two different models for describing the behaviour of the reinforcing steel or prestressing steel, namely:
- the ideal elasto-plastic model for steel with a pronounced yield range,
- the non-linear elasto-plastic model for steel without a pronounced yield range.

Any flexural stresses that may be acting in the steel are not taken into account in either model.

Ideal elasto-plastic model
It is assumed that yielding of the steel bar can occur at a crack in the concrete. Here the yield deformation of the steel is highly concentrated locally, so that in the program a delta function is used to describe the plastic strain behaviour over the length of the bar.

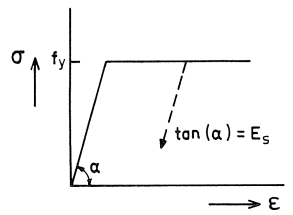

Fig. 3.27. Ideal elasto-plastic model for reinforcement.

Non-linear elasto-plastic model
The relationship between the stress (σ_s) and the strain (ε_s) is introduced for the purpose of this model. This relationship is represented in the form of a polygon.

Just as in the ideal elasto-plastic model, in the non-linear elasto-platic model the tangent modulus of stiffness on unloading is taken as equal to the tangent modulus (E_0) at the origin.

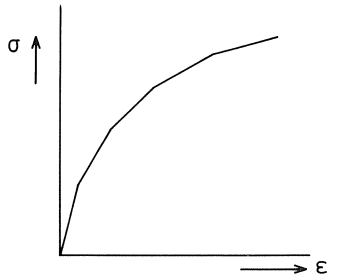

Fig. 3.28. Relationship between σ and ε in the non-linear elasto-plastic model for the reinforcement.

3.3.6 Bond characteristic and dowel action

The behaviour of the boundary layer between steel and concrete under a shear stress is described by an elasto-plastic model for the shear stress and the parallell shift $\Delta_{//}$, in-

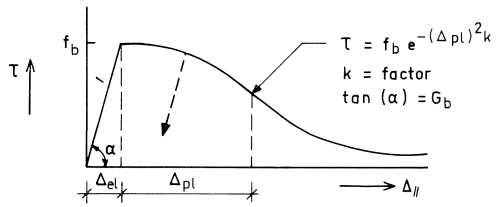

Fig. 3.29. Elasto-plastic model for bond, including softening.

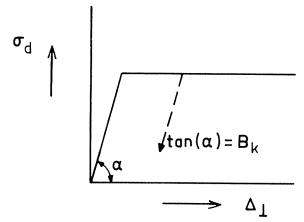

Fig. 3.30. Ideal elasto-plastic model for dowel forces.

cluding softening. The influence of the normal stress has not yet been taken into account.

Pending further research into the effect and magnitude of the dowel forces, an ideal elasto-plastic relationship between relative displacements perpendicular to the centre-line of the bar and forces acting on this centre-line has been adopted in the program.

3.4 *Numerical procedure for nonlinear analysis*

3.4.1 Initial strain method

The load can be applied in steps in such a way that results are available for a full loading path. However, the analysis is not an incremental procedure. To analyse the result for a new load step, the full load is applied. The nonlinear effect of the materials is dealt in accordance with the "initial strain method". This means that the nonlinear analysis is replaced by a linear one, in which the load vector is adapted to account for all nonlinearities. The stiffnesses for the linear part are kept constant, which makes it necessary to decompose the global stiffness matrix of the structure only once.

To work in this way, the various stress-strain relationships are all written in the form

$$\sigma = D(\varepsilon - \varepsilon^I)$$

where:

σ = stress(es)
D = initial modulus of elasticity (matrix)
ε = total strain(s)
ε^I = initial strain(s)

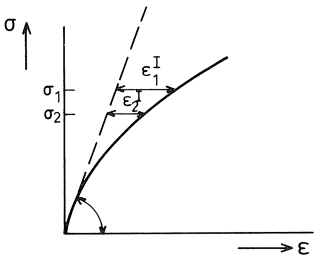

Fig. 3.31. Initial strains for two stress levels.

The value of D is chosen for $\varepsilon = 0$ (at the origin) and is kept constant in the analysis. The initial strains may be due, inter alia, to the non-linear stress-strain relationship of the concrete or the occurrence of displacements at cracks (being the three degrees of freedom which describe crack width and crack shift), but may also be caused by shrinkage and creep. An analysis by this method is based on an iterative procedure, as follows. For the first iteration the initial strains ε^I are taken as zero. For a given full external load the stresses (σ_1) at the various points of the structure are calculated. Then the initial strains (ε_1) associated with these stresses are determined from the stress-strain diagram, see Fig. 3.31. On the basis of these new initial strains the structure is again analysed for the same load. To do so, an additional load vector is composed on the basis of the new initial strains, which is summed with the full vector of external load. The resulting adapted load vector is used to calculate new displacements and stresses. Next, with the new stresses (σ_2) at the various points of the structure the initial strains (ε_2^I) associated with these are calculated. Now if the newly calculated stresses differ greatly from the previously calculated stresses, the iteration process is continued until the difference between the newly calculated stresses and those calculated in the previous iteration is sufficiently small.

How the iteration process proceeds depends on the structure and how it is loaded and supported. In a statically determinate structure only one iteration is needed to reach the exact solution. For a statically indeterminate structure more iterations are needed. The rate of convergence in this case can be increased by using a relaxation method with a relaxation factor between zero and one.

Fictitious visco-plasticity

It is a drawback of the "initial strain method" that it cannot directly be used with materials having an ideal elasto-plastic behaviour (see Fig. 3.32) because for such materials the initial strain is not uniquely defined for each stress.

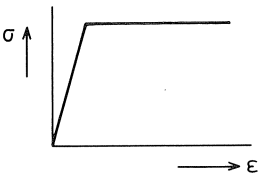

Fig. 3.32. Ideal elasto-plastic material behaviour.

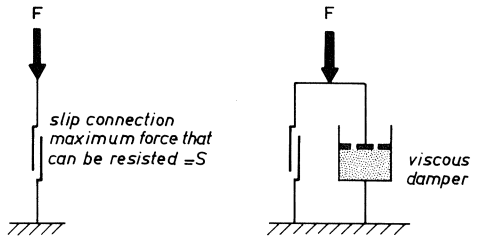

ideal plastic model visco-plastic model

Fig. 3.33. Modification of an ideal plastic model into a visco-plastic model.

For determining the initial strain of an ideal plastic material the latter is conceived as being replaced by visco-plastic material model. This means in effect that a viscous damper is connected parallel to the plastically deformable part (see Fig. 3.33).

If the visco-plastic model is loaded by a force F larger than the yielding force S, a force $F-S$ will act upon the viscous damper. The rate of strain ($\dot{\varepsilon}_{vp}$) of this damper is dependent on the load and on the viscous stiffness K:

$$\dot{\varepsilon}_{vp} = K(F-S)$$

If the iteration process is conceived as a fictitious creep process with a time interval Δt between each two successive iterations, then the increase in visco-plastic strain per iteration is:

$$\Delta \varepsilon_{vp} = \dot{\varepsilon}_{vp} \Delta t = K \Delta t (F-S)$$

The iteration process (creep process) is continued until the difference $F-S$ of the two forces has become sufficiently small. The viscous damper serves merely as a means for determining the initial strain. The viscous stiffness K and the time intervals Δt are therefore only auxiliary quantities. The magnitude of the product $K\,\Delta t$ determines whether the calculation converges and how rapidly. Carmeau, indicates what values should be adopted for $K\,\Delta t$ for the various plastic material models. In general, the process is found to converge satisfactorily if the following is conformed to:

$$\Delta \varepsilon_{vp} < \frac{2(F-S)}{D}$$

(where D is the modulus of elasticity of the material) or:

$$K\,\Delta t < \frac{2}{D}$$

A disadvantage which sometimes is attributed to the initial strain method is that it has a more restricted range of convergence than the initial stress method. The stability of the iteration process is greatly increased by ensuring that the increments of the initial strains per iteration are not taken too large. A guiding criterion for this is:

$$\Delta\varepsilon^I < \frac{\sigma}{D}$$

The concept of fictitious visco-plasticity described here is introduced in the micro-model for two aspects. It is used when a crack occurs to release the tensile stresses normal to the crack which have to drop back suddenly to zero ($S = 0$). It is also used when a yield envelope is exceeded for the plain concrete. In that case the stress has to be brought back to the relevant equivalent stress ($S = \bar{\sigma}$).

Alternative handling of cracks

It was said above that crack displacements are manipulated as initial strains, which offers the advantage that the the global stiffness relationships for the structure need then be analysed only once and that the system of equations need be decomposed only once. However, there is of course an alternative possibility. The displacements at cracks can be accommodated directly in the system of equations. This does not necessitate recalculating the stiffness relationships per element, but it will be necessary to re-establish and decompose the whole system of equations. Every time a number of cracks have formed, these are accommodated in the equations. This procedure makes for more rapid iteration.

3.4.2 Numerical procedure

We will first explain the finite element method for uncracked concrete elements. Following the notation of Grootenboer's doctoral thesis [4], all natural boundary displacements $\bar{u}$ and $\bar{v}$ and the displacements u and v in the reinforcement bar elements (see Section 3.2.2) are assembled in a vector v^0. At each loading step the full new load is applied to the structure. The set of equations which governs the behaviour of a structure can then be written in the form

$$Sv^0 = k + k_\varepsilon$$

where S is the global original stiffness matrix, k is a vector due to applied full loads and volume loads. The vector k_ε comprises the influences due to all initial strains. The derivation of the set of equations on the basis of the assumed displacement fields, stress field and material properties is not presented here. The interested reader will find the explanation in [4]. Here it may suffice to state that the set of equations is the structural generalization of the stress-strain relation which was mentioned in Section 3.4.1. This is easily seen, if we write it in another way

$$D\varepsilon = \sigma + D\varepsilon^I$$

Suppose the set of equations is satisfied for a certain full load. When a new load increment is applied, the set of equations is solved iteratively for the full new total load by adjusting the initial strains until all criteria of nonlinearity are satisfied to a certain accuracy.

Cracked state

We now envisage the situation that cracks will develop. In that case the already existing stress field with parameters β_1 is extended with an additional discontinuous stress field with parameters β_2. Apart of the already existing degrees of freedom v^0 (hereafter called v_A^0) we now have the additional degrees of freedom Δu^0 and Δv^0 at the intersection of cracks and element-edges. We assemble these additional degrees of freedom in a vector v_B^0. In [4] it is derived that the set of equations in the uncracked state now is replaced by two coupled sets of equations of the form

$$S_A v_A^0 = k_A + k_{\varepsilon_1} - k_{\beta_2}$$
$$S_B v_B^0 = k_B + k_{\varepsilon_2} - k_{v_A^0}$$

Here k_A is a vector due tot applied loads and volume loads corresponding to the displacements v_A^0, and k_B is a vector due to possible loads corresponding to the displacements v_B^0. This latter load vector is always zero.

The load vector k_{ε_1} is due to the initial strains which are linked to the already existing stress field with parameters β_1, and k_{ε_2} is a load vector due to the initial strains which are linked to the additional discontinuous stress field with parameters β_2. These initial strains include material nonlinearities, temperature effects, creep and shrinkage, but also the vector v^{cr} of the three degrees of freedom in a crack u_i, u_j, v (see Section 3.2.2). The vector k_{β_2} is calculated from the stress parameters β_2, and the vector $k_{v_A^0}$ from the displacements v_A^0. The symbols S_A and S_B represent matrices.

The split-up of the equations into two sets is done to avoid the alteration of the original system matrix S_A and the renumbering of the degrees of freedom v_A^0. During the iterative solution procedure both sets of equations are solved in sequence. In each fresh iteration, first the displacements v_A^0 are calculated with the aid of the initial strain load vector k_{ε_1}, and the secondary stress parameters β_2 from the preceding iteration. Then the displacements v_B^0 are calculated with the aid of the initial strain load vector k_{ε_2} from the preceding iteration and the newly calculated displacement v_A^0. In each iteration the initial strains ε^I (including the internal crack displacements v^{cr}) are adjusted to the criteria of non-linearity or to the stress conditions for a crack.

To take into account the internal stress redistribution due to a crack, one element crack at a time is allowed to occur. Only when the normal stresses on the crack surfaces have become sufficiently low another cracked element can occur. Each time a new crack is formed, the matrix S_B has to be formed and decomposed again. Because the bandwidth of this matrix stays very small, this requires much less time than reformation and decomposition of matrix S would take.

Initiation of cracks

To decide when an element is cracked and to determine the direction of the crack we use the average stresses over an element. When these stresses are in the range in which the crack criterion is valid and supersedes the criterion more than it does in other elements, a crack is assumed to form (with the restriction that the normal stresses on the

existing crack faces are small enough). A crack is made to pass through the centre of the triangular element, except if already a crack ends at the boundary of the element. In that case the new crack proceeds from this existing crack.

In reality there is a local stress peak near the tip of a crack. This causes further spreading of a crack, even if the average stresses in the vicinity thereof - apart from the stress peaks - are below the cracking criterion.

In the MICRO-model these highly localized stress fields are not included. The effect that, in an element adjacent to the end of an existing crack, a crack will develop at lower average stresses than it would if there were no cracks present, is here dealt with by reducing the cracking criterion for this element. The calculations that have been performed show a reduction to about 0.7 to be satisfactory.

A crack, once it has been introduced into the model, remains in existence. The procedure does, however, take account of the possibility that, on further loading or unloading the structure, it may occur that a crack closes up again by compression, but as soon as tensile stresses act across a closed crack, the latter opens again. Transfer of compressive stresses across a crack is possible only for zero crack width.

Fictitious visco-plastic approach

It has been stated in Section 3.4.1 that a fictitious visco-plastic model is used in the case of elastic plastic materials. This is so for the aggregate model in the crack and for the Buyukozturk model for concrete. By doing this, the iteration process can be conceived as a fictitious creep process with a time interval Δt between each two successive iterations and a loading of the viscous element equal to the unbalanced stresses (σ). Per iteration the increase in the internal crack displacements Δv^{cr} or initial strains $\Delta \varepsilon^I$ is:

$$\Delta v^{cr} \text{ (or } \Delta \varepsilon^I) = K \Delta t \, \sigma$$

To ensure that the iteration process is stable the value of K must not be taken too large (see Section 3.4.1). The number of iterations needed per load increment is greatly influenced by the number of cracks present in the structure.

Alternative handling of cracks

The alternative way of handling cracks, as was described in Section 3.4.1, is used whenever a certain number of cracks have formed. This accelerates the iteration process. The system matrices S_A and S_B are then changed in order to take account of the condition that the normal stresses on the faces of open cracks must become zero.

3.4.3 The MICRO/1 program

The MICRO/1 program operates as a so-called subsystem under the control of the Genesys system and is programmed in the Gentran language, a dialect of Fortran. Input of this program is done with tables and commands which are defined in the Genesys manner and which can be stated unformatted.

The numbering of the degrees of freedom and the manner of solving the ultimate sys-

tem of equations are based on the wave front method. The modified Crout algorithm is used for solving the system of equations. This algorithm is so programmed that during decomposition only the system triangle is present in the working storage. The output is selective and may take the form of tables and/or diagrams. Fig. 3.34 presents an overall flowchart.

Special feature

The program allows for scatter in the tensile strength of concrete and in the bond strength. Particularly for concrete it is true to say that its composition is liable to vary from one point to another in a structure. In the program each element will (if desired) be assigned a different tensile strength. This results in a realistic distribution of crack spacings and crack widths in a state of homogeneous stress.

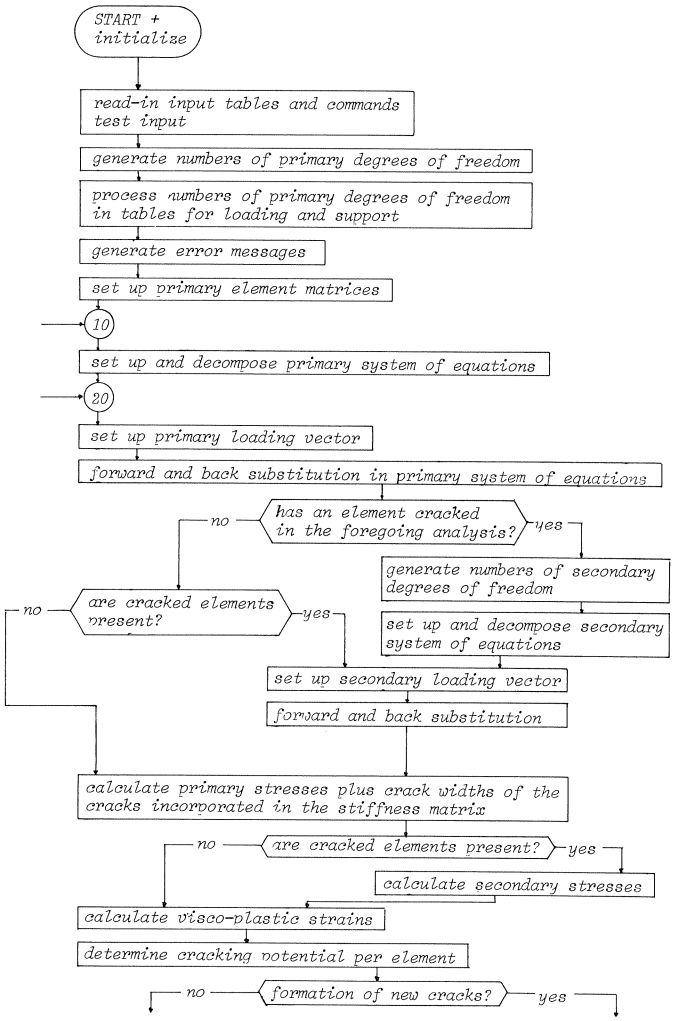

Fig. 3.34a. Overall flowchart of the MICRO program.

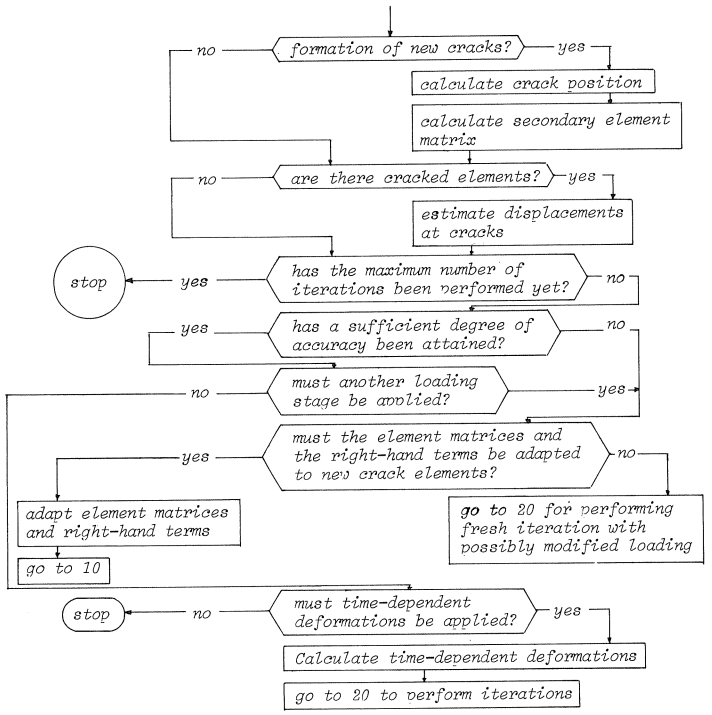

Fig. 3.34b. Continuation of overall flowchart of the MICRO program.

4 Verification and application examples

In order to test the MICRO-model with regard to its serviceability and ability to meet the objectives, a number of structures whose experimental behaviour has been described in the literature were analysed with the aid of the model. Since only a limited number of analyses were performed, it was not practicable to check all the possibilities of the model. In the analyses the time-dependent behaviour and the behaviour under alternating load were not considered. Although the possibile occurrence of dowel forces in the reinforcement and of parallel displacement at a crack was allowed for in the model, neither of these phenomena occurred to any significant extent in the structures analysed.

If possible, the analyses have been performed in a displacement-controlled way. Just as in performing an experiment, an analysis based on a prescribed displacement offers advantages in comparison with an analysis based on a prescribed loading. Thus, in the prescribed displacement method any retrograde changes in the load-deflection diagram can be detected, whereas this is not possible in an analysis based on a prescribed loading. Also, the first-mentioned method is advantageous in a case where the structure develops ideally plastic or very nearly ideally plastic behaviour. In an analysis based on a prescribed displacement the iteration process will, in such a case, still converge rea-

sonably rapidly, whereas in the prescribed loading method there will be very poor convergence or indeed none at all.

Unfortunately, an analysis based on a prescribed displacement is not always possible. If a structure is subjected to a number of point loads or a uniformly distributed load which are of variable magnitude, it will be necessary to perform the analysis with a prescribed magnitude of the loading.

In the following sections results will be presented of some of the analyses performed. The first example is the simulation of a part of a beam in a state of constant moment. The next example is a plate in a state of plane stress, with a small couple of heavy cracks dominating the behaviour. The third example shows how beam failure in shear can be appropriately predicted. And finally the subject of a fourth example is the analysis of a beam-to-column connection.

The second example (plate in plane stress) and the third example (beam failing in shear) relate to structures in which one or two discrete cracks dominate the behaviour of the structure. Such problems cannot be modelled satisfactorily with "smeared-out" cracks. The MICRO/1 program does cover these phenomena, however.

4.1 *Beam subjected to pure bending*

One condition for succesfully employing a computer program for the analysis of structures having a complex internal pattern of forces is that a numerical model of his kind should correctly analyse the basic cases with regard to loadbearing capacity. One such a basic case to be analysed is a reinforced concrete beam loaded in bending. The beam chosen is one of a series of beams with varying percentages of reinforcement and subjected to four-point loading tests as reported in [10]. The beam selected for the present purpose was No. 8 with a proportion of tensile reinforcement equivalent to 0.47% of the cross-sectional area of the beam. The dimensions of this test specimen and the manner of loading are indicated in Fig. 4.1.

In order not to have to consider the effect of shear force in this analysis, the latter was confined to the behaviour of the region between the two point loads, where the bending moment is constant.

For analysing the behaviour in pure bending it will suffice to consider only a short portion of the beam. This portion should, however, be chosen sufficiently large to ensure that several cracks will develop in it, so that both the state of stress at a crack and the state of stress between two cracks are comprised in the analysis. Accordingly, for an

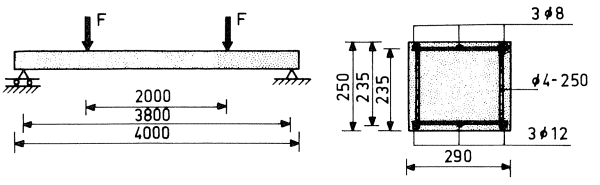

Fig. 4.1. Test on beam for constant moment (dimensions mm).

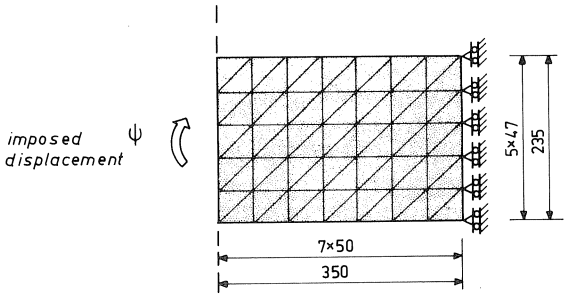

Fig. 4.2. Element mesh.

expected maximum crack spacing of 140 mm, a 350 mm long portion of beam was adopted for the analysis.

At its left-hand end this portion is loaded with a prescribed angular rotation ψ, whereas rotation is prevented at the right-hand end (Fig. 4.2). The effect of the concrete cover to the bottom reinforcement has not been taken into account in the analysis. This omission can result in 13% over-estimation of the concrete stresses in the uncracked beam. When cracks develop in the beam, however, the effect of ignoring the bottom cover is negligible. The element mesh is shown in Fig. 4.2.

Furthermore, the analysis has been based on the under-mentioned material properties, as reported in [10]. The properties of the boundary layer between steel and concrete have been estimated.

Concrete: non-linear behaviour: Link's model

$f_c = -31.1$ N/mm^2
$f_{ct} = 3.75$ N/mm^2
$E_c = 30000.$ N/mm^2
$\nu_c = 0$

Steel: ideal elasto-plastic model

$f_y = 441.$ N/mm^2
$E_s = 218500.$ N/mm^2

Bond:

$f_b = 3.75$ N/mm^2
$G_b = 3500.$ N/mm^3

Typical results of the analysis are found in Fig. 4.3 and Fig. 4.4. In the first one the curvature, the maximum crack width and the stresses in the reinforcement and in the concrete are compared with the experimental results. The bending moment at which the first crack occurs is 10 kNm in the experiment and 11 kNm in the analysis. Whenever a crack is formed, there is, according to the analysis, a slight decrease in the magnitude of the moment for a somewhat greater angular rotation. These decreases in bending moment are not manifest in the experiment because it was performed under

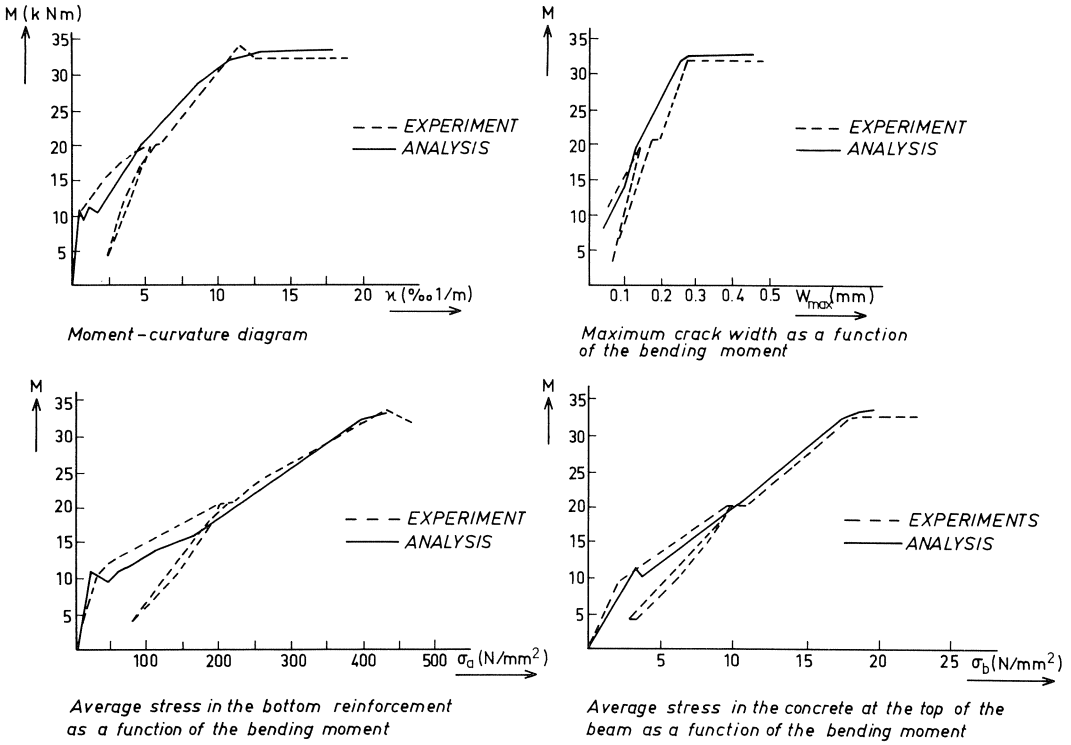

Fig. 4.3. Typical results of MICRO/1 for a constant moment area in a beam.

load-controlled conditions. The bending moment at which yielding of the tensile reinforcement occurs is 32 kNm in the experiment and 33.5 kNm in the analysis.

The relations between the average (tensile) stress in the bottom reinforcement and the bending moment as determined in the experiment and in the analysis are reasonably similar. On comparing experiment and analysis, the abrupt increase in the average steel stress as calculated in the analysis after the occurrence of the first crack is notable. The difference between experiment and analysis is due to the fact that in the experiment a longer portion of the beam is considered and the cracks do not occur at the same load but develop only gradually between a moment of 10 kNm and 24 kNm. In the analysis, on the other hand, all big flexural cracks occur at the same bending moment of 11 kNm. The fact that in the experiment these cracks do not all occur at the same load must be due to internal scatter (variation) in the tensile strength of the concrete and/or to scatter in the bond between concrete and steel.

The effect of this scatter manifests itself not only in the differences in bending moment at which the cracks occur, but also in the scatter in the crack spacings. The crack patterns obtained experimentally and by analysis, at a load at which yielding of the bottom reinforcement occurs, are shown in Fig. 4.4. The distances between the big flexural cracks are in good agreement with each other, which makes us suppose that the

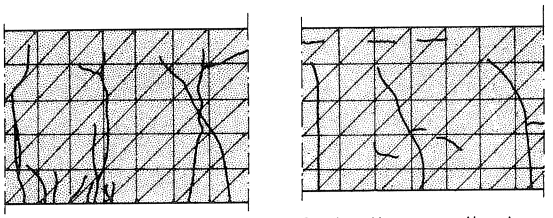

Fig. 4.4. Crack pattern associated with yielding of the bottom reinforcement.

chosen values for bond are of the proper order of magnitude. In the experiment a couple of short additional cracks occur which do not occur in the analysis. This may be due to scatter in the material properties in the experiment. Other analyses (not reported here) also produce the short cracks, however.

From the comparison of analysis and experiment it appears that the behaviour of a beam loaded in bending can be satisfactorily analysed with the Micro-model. In making this comparison, much attention has been paid to the differences between the calculated and the experimentally determined results in consequence of the scatter in the actual material properties. This scatter, however, has little effect on the overall behaviour and on the magnitude of the steel and concrete stresses. It is significant only in so far as the average crack spacing and crack widths are concerned. The homogeneous material model gives good results for the maximum crack spacing and maximum crack widths.

4.2 *Plate in plane stress*

In Section 1.3 was stated, as one of the aims of the Micro-model, that this model should be suitable for the analysis of structures in which only few dominant cracks determine the behaviour. The reason for this aim is that models with "smeared-out" cracks do not do sufficient justice to these dominant cracks. An example of a structure in which only a few dominant cracks determine the behaviour is the plate WT2 in the series of tests on various types of plate structure described by Leonhardt and Walther in [11]. The plate in question is loaded along its upper edge, as shown in Fig. 4.5. Noticing the position of the cracks, it is to be expected that not much shear stresses will develop in the cracks. In this problem the bond data will be of more importance than the data for aggregate interlock.

On account of symmetry of the structure and of the boundary conditions, it is sufficient to confine the analysis to one half of the structure. For analysing the half plate the boundary condition on the right-hand side is the symmetry condition that the horizontal displacement of the plate midway between the two bearings must be zero.

The network of elements for the concrete and for the reinforcing bars, respectively, is indicated in Fig. 4.6, as well as the manner of loading and support.

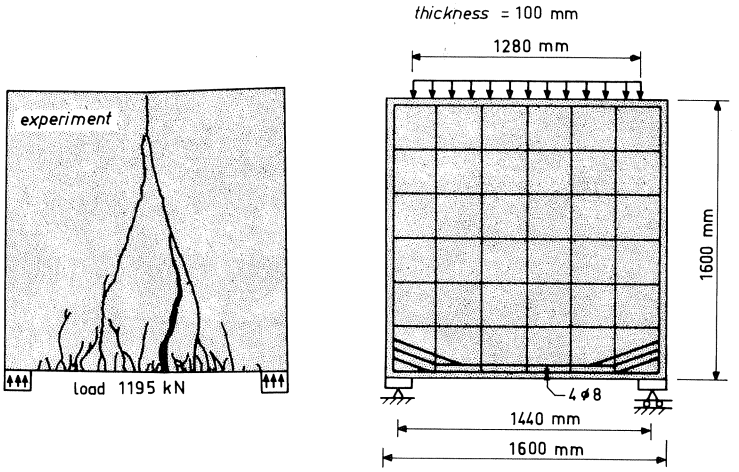

Fig. 4.5. Crack pattern and reinforcement in plate loaded on top.

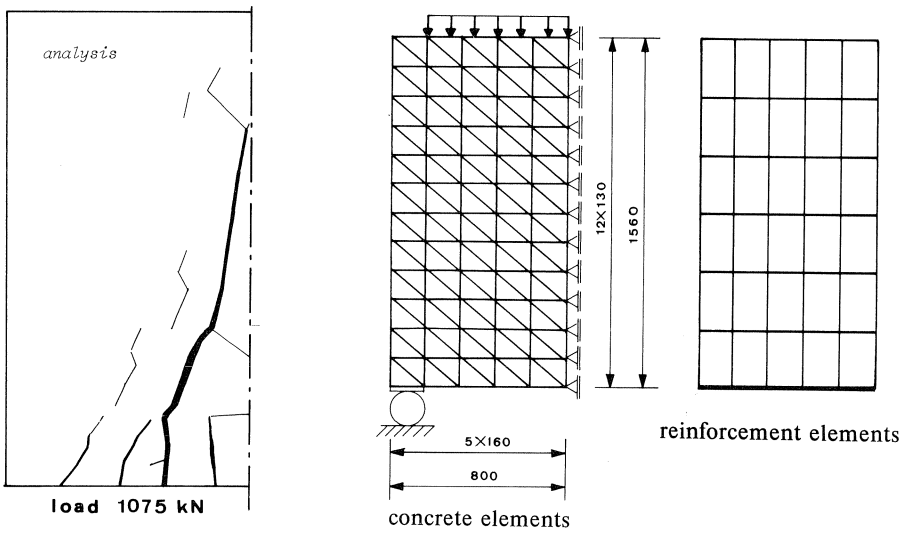

Fig. 4.6. Crack pattern and element mesh in analysis of plate loaded on top.

Since the structure is subjected to a uniformly distributed load, the analysis had to be performed with a stepwise increasing load applied to the top of the plate. The following material properties have been adopted in the analysis:

Concrete: non-linear behaviour: Link's model

$f_c = -30.1$ N/mm^2

$f_{ct} = 3.5$ N/mm^2

$E_c = 32000.$ N/mm^2

$\nu_c = 0.2$

Steel: non linear elasto-plastic model
$E_s = 210000.$ N/mm^2
$f_y = 400.$ N/mm^2 (some hardening)

Bond: $f_b = 4.7$ N/mm^2
$G_b = 47.$ N/mm^3

The result of the analysis for the crack pattern is shown in Fig. 4.6. In Fig. 4.7 the results for the stress σ_s in the bottom reinforcement and the maximum crack width are compared.

It is very gratifying to find that the MICRO/1 program produces one dominant crack per half of the structure. This seems to be a major step forward in the analysis of structures in which such phenomena occur. Analysis and experiment both reveal only a few dominant cracks which start at the bottom of the plate, between the axis of symmetry and the support, and which in the upward direction bend towards the centre of the plate. It is the feature of bond slip which makes it possible that large crack widths develop. The analytically calculated width of the cracks is likewise in sufficiently good agreement with the measured widths. It does, however, emerge from the crack pattern determined by analysis and by experiment, respectively, that the number of elements in the analysis is too small to describe the correct crack spacing in the bottom edge of the plate.

Since the number of smaller cracks which would develop at the bottom edge of the plate have only little effect on the overall behaviour, the load-deflection curves accord-

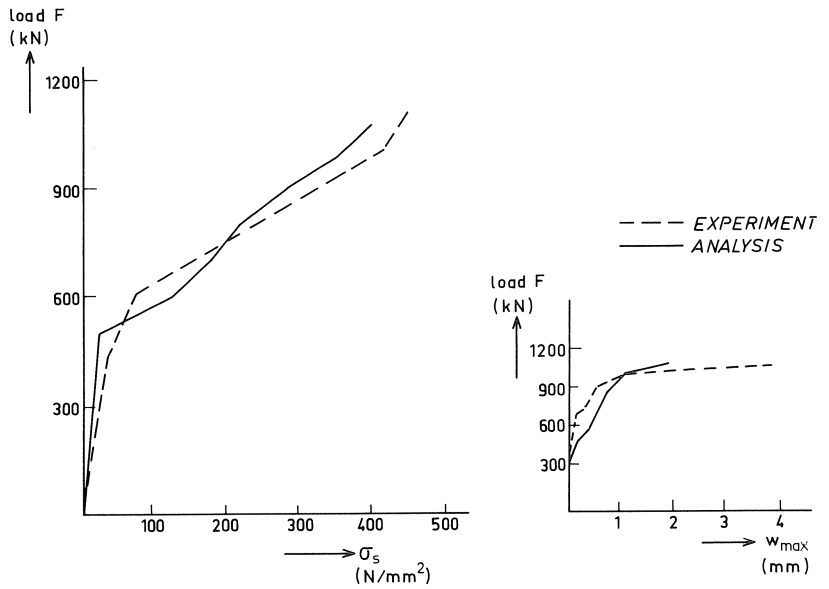

Fig. 4.7. Stress in bottom reinforcement on axis of symmetry and maximum crack width in plate loaded on top.

ing to experiment and according to analysis are in excellent agreement (not shown here).

The steel stress also is in very good agreement with the results of the experiment. This is more or less to be expected if the crack pattern is similar in the experiment and in the analysis. The steel stress is determined by the cantilever arm between the compression zone and the bottom reinforcement, and this arm is almost the same in the experiment and the analysis.

The maximum crack width w_{max} is strongly dependent on the number of cracks that will occur and of the assumed bond data. The sequence in which the cracks come into being is also important. Taking account of these considerations, the agreement between the experiment and the analysis is reasonable.

4.3 *Beam failing in shear*

One might say that the examples in Section 4.1 and 4.2 have proved the ability of MICRO/1 to simulate bending failure. We now consider a reinforced concrete beam which fails in shear. This beam is one of a series of beams which were tested in the Stevin Laboratory of the Delft University of Technology in the Netherlands in a program of research to investigate the influence of beam depth and crack roughness on the shear failure load [12]. The beam was loaded as shown in Fig. 4.8.

On account of symmetry of the structure, the boundary conditions and the loading, it was sufficient to confine the analysis to one half of the structure. The network of elements, the restraints and support and the external loading of this half structure have been shown in Fig. 4.9.

The experimentally determined failure load and the failure load found from the analysis were very close to each other (112.1 kN and 112.4 kN). The load-deflection curves for the experiment and the analysis are given in Fig. 4.10.

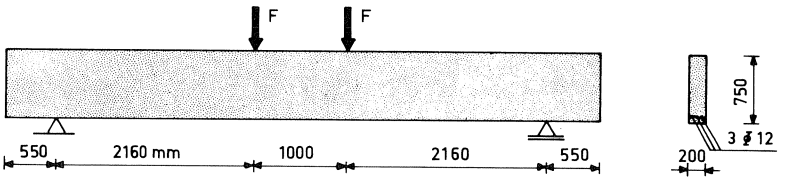

Fig. 4.8. Shape of tested beam and manner of loading.

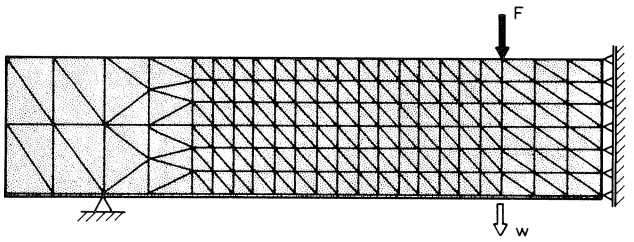

Fig. 4.9. Network of elements.

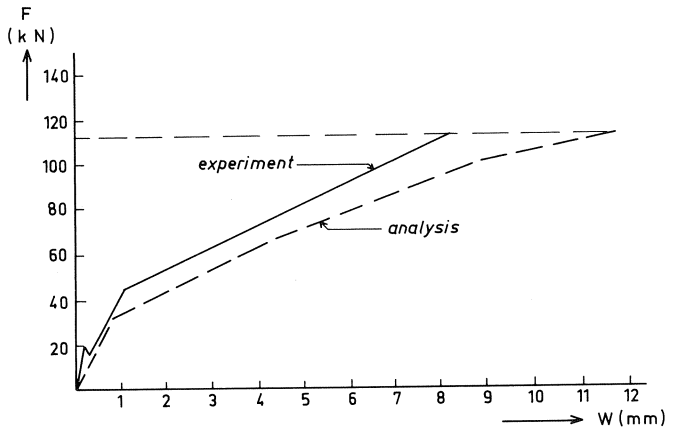

Fig. 4.10. Diagram of load F and deflection w.

It follows from the load-deflection curves that the analysis leads to a somewhat lower stiffness than was registrered in the experiment. An explanation for this lower stiffness may be too low a tensile strength for the concrete in the analysis, which results in the premature occurrence of cracks and a bend in the load-deflection curve at a lower value of the load than in the test. The maximum bond-stress between steel and concrete may have been chosen too low as well.

Fig. 4.11 shows the crack patterns just before failure, according to experiment and analysis. In the experiment as well as in the analysis abrupt failure occurred, caused by crushing of the concrete at the tip of an inclined (shear) crack. Now the analysis also pro-

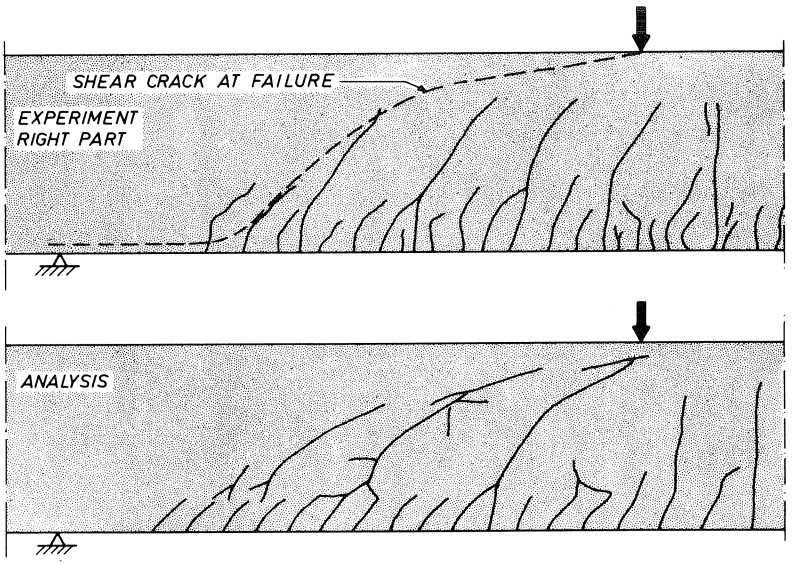

Fig. 4.11. Crack pattern in experiment and analysis.

duces the short cracks which occur in the tension zone between the major cracks which run into the compression zone. The agreement between the crack patterns is remarkable indeed. That failure is due to shear in this case is once more supported by the fact that the reinforcing bars in the tension zone were still below the yield stress.

4.4 *Beam-to-column connection*

A beam-to-column connection is a structural feature in which a combined state of normal force, bending moment and shear force occurs. This will clearly be reflected in the crack pattern that develops. A structure has been analysed which was investigated in the Stevin Laboratory in a program of research on the strength and rigidity of various types of beam-to-column connections.

These tests are more particularly of interest because they showed these specimens to fail at a lower value of the load than had been anticipated on the basis of the failure loads of the sections of the beam and of the connected columns. Test specimen No. 1402 in this series of beam-to-column connections described in [13] has been analysed. The structural dimensioning and the manner of loading and support are shown in Fig. 4.12.

For details of the analysis, see [4]. Here we want to demonstrate the possibilities of the MICRO/1 program. The failure load in the analysis ($F_u = 61{,}5$ kN) corresponds rather well to the failure load in the experiment ($F_u = 65.3$ kN). The load-deflection curve (not shown here) is in very good agreement with the analysis. The analysis was terminated at 7 mm deflection of the beam, because for this value the analysis indicates that crushing occurs in the concrete in the compressive zone of the lower column directly under the beam. Such crushing in that region is also found to occur in the test specimen. A number of typical results is shown in Fig. 4.13. The crack patterns correspond quite well. Both the experiment and the analysis reveal diagonal shear cracks which develop in the connection.

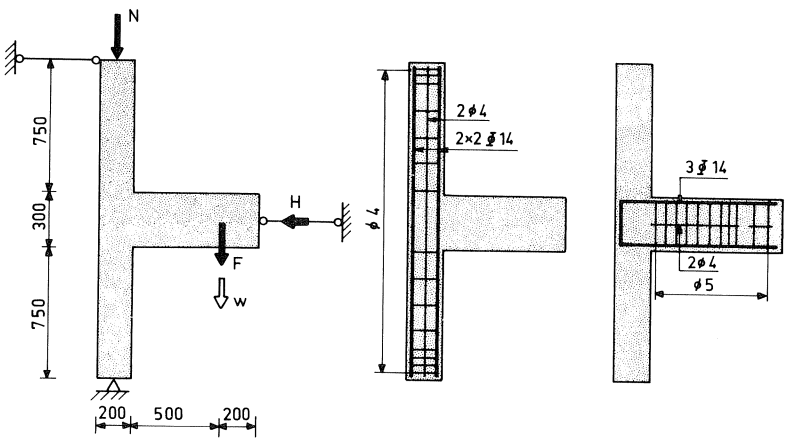

Fig. 4.12. Loading, support and reinforcement of beam-to-column connection.

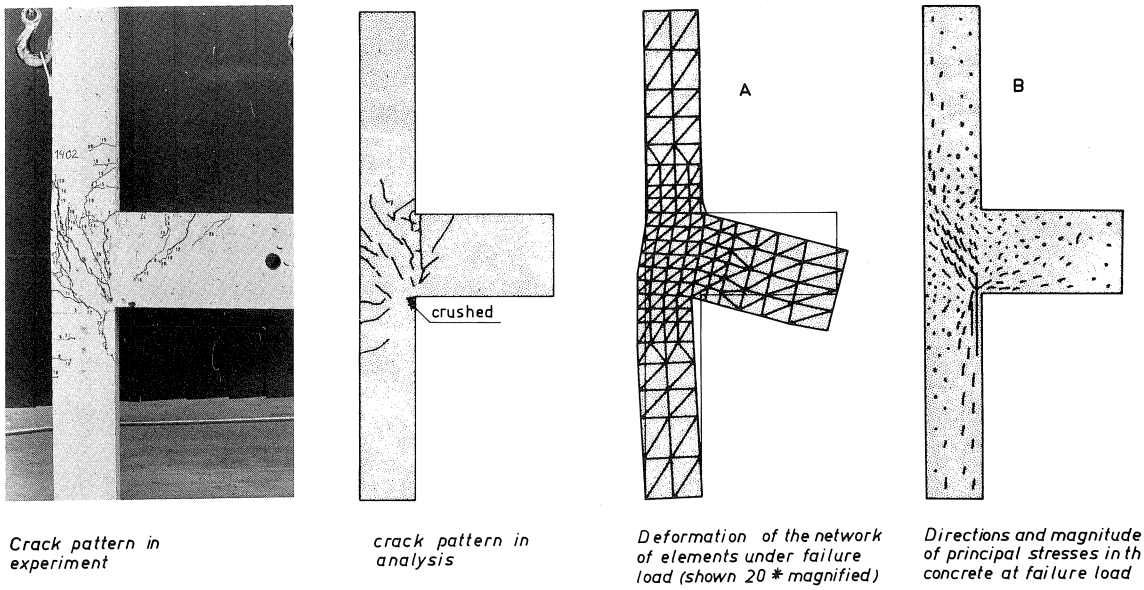

Fig. 4.13. Typical results for a beam to column connection.

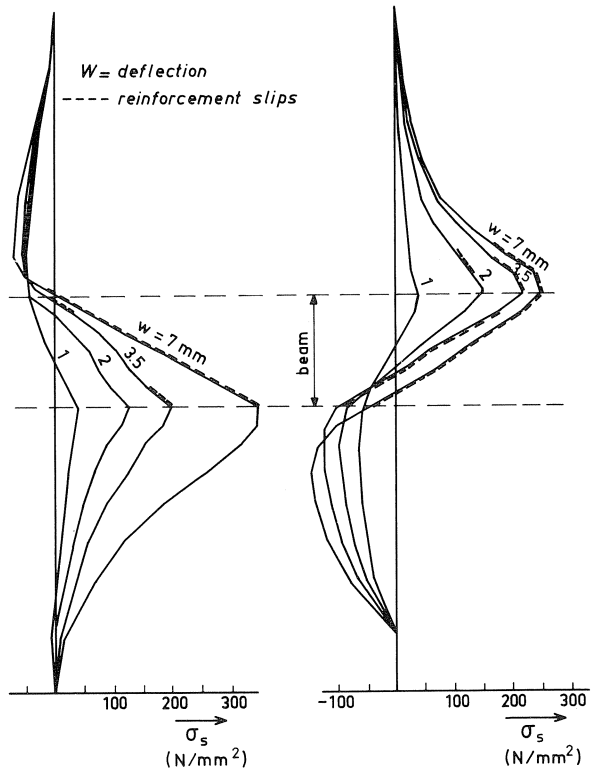

Fig. 4.14. Stresses in column rebars.

It was very satisfactory to find that MICRO/1 succeeded in simulating some special fact which occurred in the experiment. The two bending moments applied by the two column parts to the connection are equal in the uncracked state, but start differing when cracks develop. At the failure load this distribution is in the proportions of 31% (upper column) and 69% (lower column) in the experiment. The analysis did not produce the same figures, but demonstrated substantially the same effect (40% and 60%).

The potential of the MICRO/1 program may be underlined by one more special result. The vertical bars in the column and the horizontal bars in the beam are found to slip in the connection area when the deflection w of the beam end exceeds 3.5 mm.

Apparently the length of the reinforcing bars in the connection region is too short for the rather abrupt change of the stresses in the bars. The calculated stress σ_s for the column reinforcement is presented in Fig. 4.14.

The right-hand diagram in Fig. 4.14 relates to the bar nearest to the beam. It is easily seen that the steel stress do not change very much when the deflection w increases from 3.5 mm to the double value of 7.0 mm. This bar slips over the total length of the connection area and in part of the upper column. The steel stress therefore does not reach the yield stress. A similar effect has been observed in the beam bars. This is a major reason why the connection fails at a lower value of the load than had been anticipated on the basis of the failure loads of the sections of the beam and the column.

5 Conclusions and work ahead

As stated in Chapter 2, the aim of the Micro-model has been the development of a tool with which the behaviour of two-dimensional structures in plane stress can be analysed. This behaviour to be analysed comprises:

- the deformation of the structure at a particular magnitude of the load;
- the magnitude of the load at which cracks are formed in the structure;
- the crack spacing and crack widths;
- the slip of the reinforcement;
- the stresses in the concrete and in the reinforcing steel at a particular magnitude of the load;
- the magnitude of the failure load.

In the analysis it is necessary to take account of the non-linear and possibly time-dependent behaviour of concrete, the non-linear behaviour of steel, the non-linear behaviour in the zone of contact between these two materials, and the possibility of transfer of stress across a crack in the concrete.

Conclusions

On comparing the results of analyses with those of experiments it appears that the Micro-model can provide a good insight into the above-mentioned behaviour characteristics. This is true both of structures with fairly well distributed cracking and of structures with only a few dominant cracks. From the analysis of the beam-to-column con-

nection it emerges that the slip of the reinforcement is of major influence upon the internal stress distribution, the magnitude of the failure load and the deformation of the structure. Also the development of a few dominant cracks, with large widths, in the plate loaded at its upper edge is possible only because the bottom reinforcement in this plate can slip in relation to the concrete. The slip of the reinforcing steel as well as the associated development of dominant cracks are well reproduced in the analyses.

From the results of the analyses it furthermore appears that the elements developed on the basis of the hybrid method with natural boundary displacements provide a good insight into the stresses and deformations even if the structure is divided into a limited number of elements.

The scatter of the tensile strength of the concrete in the structure is found to be of major influence on the scatter in the crack widths and crack spacings. On the other hand, the effect of this scatter in the tensile strength upon the overall deformation of the structure is not significant.

When a number of identical experiments are performed, the scatter in the measured crack widths will, however, likewise be greater than the scatter in the deformation.

On judging the differences between experiment and analysis it is necessary to take account of this scatter. An analysis based on the assumption that the tensile strength of the concrete does not vary from one part of the structure to another will suffice only if the object of the analysis is to obtain insight into the deformation, the average crack width and the average crack spacing.

The method adopted in the analyses, where the elements at the end of a crack will undergo cracking at lower stresses than elements not so situated, gives values for the crack penetration depth which are in good agreement with reality. It also appears that the continuity of the cracks in the analysis agrees well with the experimentally determined cracking behaviour.

Work ahead

The satisfactory performance of the Micro-model with regard to the results presented here does not mean that this model or the material models employed do not require any further refinement. We shall list a number of arguments in support of continuing along this line of research.

First of all, since only a limited number of structures has been analysed, not all the possibilities of the model have been tested to an equal degree. Especially dowel action was absent in the structures analysed.

The data for aggregate interlock and bond which have been applied in the several analyses were chosen on the basis of engineering judgement and furthermore so as to map the experimental investigations in the best possible way. The values used are in the range which is not a variance with information found in existing literature. The choice of these data can be improved in the future by using the results of project 1 of "Betonmechanica" in which the transfer of forces in cracks has been studied and the results of project 2 for the bond zone. The integration of these results in the Micro-model will not

only mean that the material data are better estimated. In fact, the more refined idealizations of the aggregate zone and the bond zone as shown in Section 3.1 must replace the actually chosen preliminary models of Section 3.2.

The recent Micro-model has been developed for monotonically increasing loading. Unloading of material along a different path than loading has not been considered yet. In general, cyclic loading could be a good extension of the program.

The Micro-model as reported here provides facilities for creep and shrinkage based on CEB report 111, dating from 1975. More insight in this problem field has meanwhile been gained indicating that it is necessary to take account of the moisture process in the concrete to define the coupled phenomenon of creep and shrinkage properly. It is worth considering integration of the (so called) "Munich model" in the Micro-model to achieve this purpose.

It must be borne in mind that the Micro-model has been developed for plane stress problems. Many problems, especially details of large structures, however, must be treated, as three-dimensional states of stress. It may not be too difficult to prepare a Micro-model for cases in which both the structure and the loading are axisymmetric. A major change of the Micro-model would be needed, however, to make it applicable to any general three-dimensional problem. This effort may even be an order of magnitude more complex than the existing two-dimensional version of the Micro-model.

Finally, one may question the basic assumption of the Micro-model that no large displacements occur, allowing a linear relation between strains and displacements to be adopted. The occurrence of wide cracks could raise the question whether displacements will become large. The results gained until now in no way support such an idea, however. If test results do show extreme displacements of (parts of) a structure after the occurrence of one dominant and fatal crack, these extreme displacements do not occur until the failure load is reached. So they develop only in the very final stage which comes after the point up to which the Micro-model is of value.

MACRO-MODEL

6 Scope of Macro-model

The Genesys subsystem STANIL/1 is a program according to the finite element method based on displacements, for the nonlinear analysis of displacements and stresses in structures consisting of reinforced concrete beams and columns. The structures are assumed to show an elastic behaviour and to be statically loaded. Geometrical nonlinearities are taken into account.The STANIL/1 program is an extension to an existing program which was reported in 1972 [14]. That program was based on the concept of a so called layered beam element, a concept that was used in parallel studies by other investigators.

The element gives very good results for load combinations of pure bending and axial forces. However, the influence of shear forces could not be simulated adequately, and no bond slip was taken into account. These problems have been solved in the new program STANIL/1 now presented, which uses a beam element taking shear deformations and the action of vertical stirrups into account as well. The full theory of this program is reported in [5].

Applications of the STANIL/1 program are found in investigating:

- the ultimate bearing capacity of reinforced concrete beam/column structures;
- the failure mode when the ultimate bearing capacity is reached (for example "bending failure" or "shear failure") as well as the deformation capacity at failure (ductile or brittle);
- the stiffness of structures after the occurrence of cracks and the influence of cracking on the stability of structures.

It is proper to state here, however, that the *corner connections* between beams and columns are *not adequately* accounted for in the existing version of the program. The corner connections between beams and columns are considered to be perfect, which is not always the case in practice.

Some of the facilities the now available STANIL/1 program offers are:

- the shape of the cross-section of a beam or column may be prismatic or nonprismatic (though symmetric to the plane of the structure);
- elements may be connected to the nodes by hinges;
- spring supports whose force-displacement characteristics may be nonlinear (elastic);
- choice of iteration method;
- graphical output of stresses and inclinations of cracks.

Integration with other subprojects

It was indicated in the Preface that the intention of the "Betonmechanica" project

is to incorporate the basic models in the global models. In order not to delay the development of the global models, preliminary choices based on what was known from the literature were made for the basic models. At the moment the final reports of projects 1, 2 and 4 are awaited. The implementation of the results in the Macro-model will then take place. The Macro-model presented in this report does not yet contain the results of the other projects.

7 Outline of theory of Macro-model

7.1 *Physical phenomena to be modelled and schematization of geometry*

The principles of STANIL/1 can easily be explained by considering a simple test beam supported at the ends and loaded by two concentrated forces. The beam is inspected at a stage where considerable formation of cracks has occurred.

In the pure bending area of the beam the deformations are restricted to axial strains in both concrete and longitudinal reinforcement (Fig. 7.1). For finite element analysis it is convenient to make a distinction between the curvature κ_{xx} and the axial strain e_{xx}.

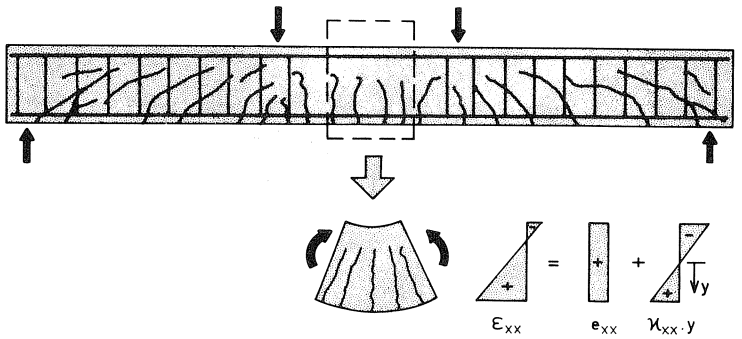

Fig. 7.1. In the pure bending area the deformations are restricted to axial strains in both concrete and longitudinal reinforcement.

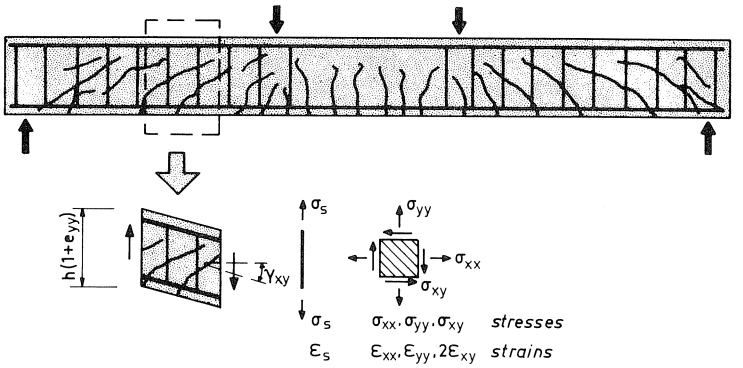

Fig. 7.2. In the shear span of the beam the concrete is subjected to a two-dimensional stress (strain) state.

In the shear span of the beam diagonal cracks may occur (Fig. 7.2), causing elongation of the stirrups. The concrete in the shear span is, apart from axial strains, also subject to a vertical deformation e_{yy} (in the direction of the stirrups) and a shear deformation y_{xy}. It is essential to realise that the concrete is subjected to a two-dimensional state of stress (strain).

The basic idea behind the beam element used in STANIL/1 is, that the element should be capable of simulating every possible two-dimensional stress (strain) situation. Moreover, only one element is used over the depth of (for example) a girder.

Modelling of the physical behaviour of a structure

How a structure is schematized in order to be able to analyse it with STANIL/1 will be illustrated by an example of a simple test beam. Because of symmetry only half the structure has to be considered (Fig. 7.3). The reinforced concrete structure is divided into a number of elements; in this example four elements are chosen.

The longitudinal reinforcement is smeared out into two thin sheets, each having the same cross-section (mm^2) as the actual reinforcement. The stirrups in an element are smeared out over the full length of the element. In the front view of the element an imaginary grid is placed; a grid line extending in the direction of the axis of the element is called a *fibre*, while a grid line which is perpendicular to the axis of the element is called a *section*. The behaviour of the element is derived from the behaviour of a number of sections. The behaviour of a section is derived from the behaviour of a number of fibres in that section.

The material properties may, depending on the stress-strain situation, be different at each point of the grid. The material properties of a fibre are considered to be representative for a *layer* on both sides of the fibre concerned. Therefore this type of element is often referred to as a *layered beam element*. The behaviour of a section is found by appropriately summing the behaviour of each separate layer.

Cracking of concrete is taken into account by modifying the material properties. In

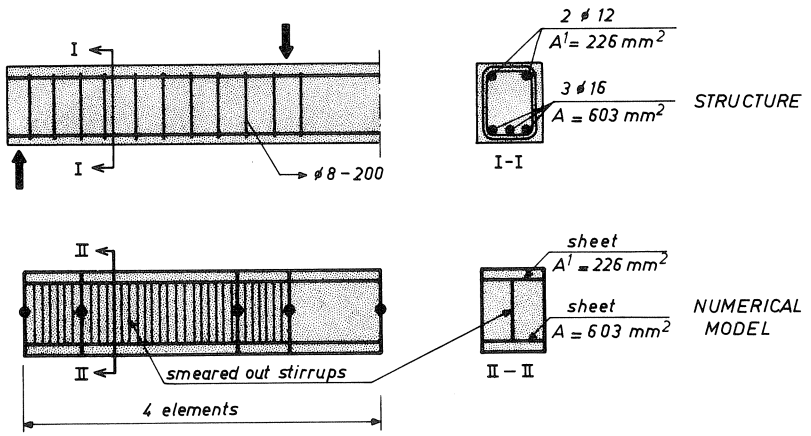

Fig. 7.3. Schematising the structure to a numerical model.

this approach the occurrence of discrete cracks is simulated by replacing the cracked concrete by a fictitious homogeneous material with properties which represent a relation between average stresses and average strains in cracked concrete.

How the element can be made to simulate every possible two-dimensional state of stress (strain) will be indicated in Section 7.2. The relations between stresses and strains which are used in STANIL/1, will be described in Section 7.3.

The mathematical procedure adopted in the nonlinear analysis will be explained in Section 7.4.

7.2 *Analytical modelling*

In order to ensure that every possible two-dimensional state of stress (strain) which may occur in a beam (column) structure can be simulated, a field of displacements is chosen, allowing the following deformations to occur:

- deformation of concrete and longitudinal reinforcement by normal force (axial deformation) and bending moment (curvature);
- deformation of concrete by shear force and elongation of the stirrups;
- slip of the longitudinal reinforcement with respect to the surrounding concrete.

By allowing these deformations to occur, it can be presumed that truss action in a beam can be simulated, in which case concrete diagonals and vertical hangers are needed.

The choice which was made for the distributions of the various deformations will be described below.

Deformation of concrete by normal force and bending moment

The field of displacements is so chosen that the axial deformation e_{xx} and the curvature κ_{xx} may vary linearly along the axis of the element. For this a total of 7 degrees of freedom is needed (u_1^c, u_2^c, u_3^c and w_1, w_2, φ_1, φ_2), see Fig. 7.4.

Deformation of concrete by shear force and tensile strain in stirrups

The field of displacements is so chosen that the shear deformation γ_{xy} and the tensile strain in the stirrups e_s may vary linearly along the axis of the element, for which another 4 degrees of freedom are needed (γ_1, γ_2 and Δh_1, Δh_2), see Fig. 7.5. The bond between concrete and stirrups is assumed to be negligable.

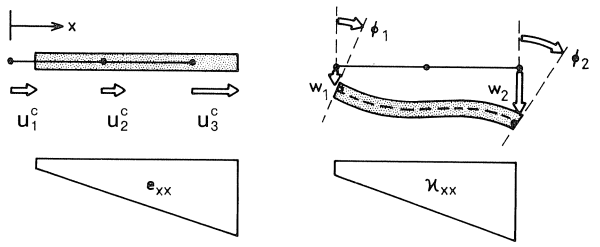

Fig. 7.4. Degrees of freedom and deformations for axial strain e_{xx} and curvature κ_{xx}.

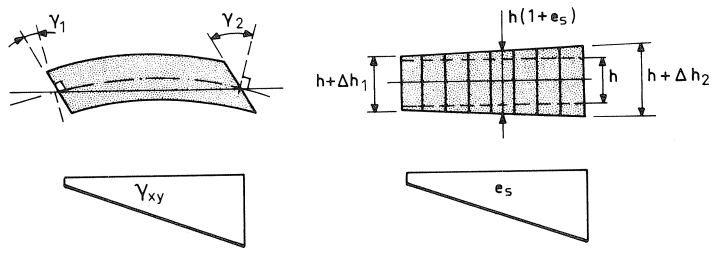

Fig. 7.5. Degrees of freedom and deformations for shear γ_{xy} and strain in stirrups e_s.

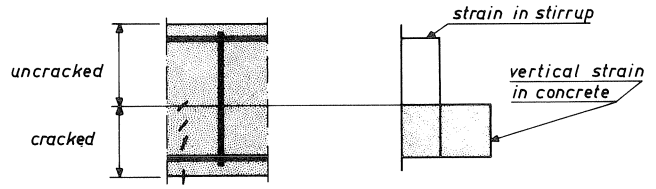

Fig. 7.6. Distribution of the vertical strains in a section of the beam element.

The vertical strain in concrete e_{yy} is also derived from the strain in the stirrups e_s. It is assumed that vertical strains in concrete only occur in that part of concrete which is cracked (see Fig. 7.6).

Slip of longitudinal reinforcement with respect to the surrounding concrete

In the beam element of STANIL/1 there occurs interaction between concrete and longitudinal reinforcement. This interaction is achieved as follows. Around the reinforcement bars a tubular bond spring is imagined which represents the contact zone between the concrete and the reinforcement. Besides the above-mentioned field of displacements u^c for axial displacements of concrete (degrees of freedom u_1^c, u_2^c and u_3^c) a separate field of displacements u^r is chosen for the longitudinal reinforcement. The distribution of u^r along the axis of the element is quadratic (just as u^c). The relative displacement (slip) of the bond spring is found as the difference between the displacements of the reinforcement and the concrete, resulting in three additional degrees of freedom (Δu_1, Δu_2, Δu_3). For both bottom and top reinforcement 6 extra degrees of freedom are necessary.

From experience gained in testing the Macro-model it was learnt, however, that it is preferable to ensure *a priori* that the difference of the displacements between steel and concrete (slip) only varies linearly (see Fig. 7.7).

The anchorage zone of the longitudinal reinforcement (at the end of a beam or column) is in fact a complicated three-dimensional stress (strain) problem. In STANIL/1 this is schematized by adding an extra point spring between the end of the reinforcement and the concrete at that place.

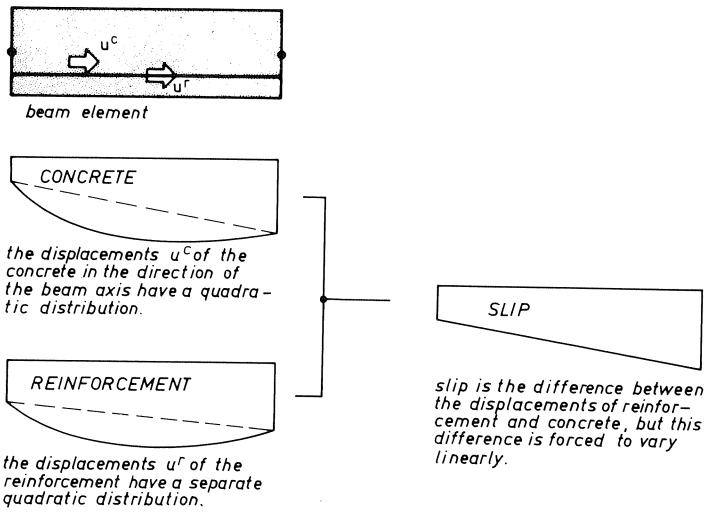

Fig. 7.7. Modelling of the slip of the longitudinal reinforcement with respect to the surrounding concrete.

7.3. *Material properties*

In the previous section it was indicated which deformations are taken into account in STANIL/1. These deformations have corresponding stresses. The relations between stresses and strains which are used in STANIL/1 will be described below.

Beforehand it should be noted that no time-dependent effects are taken into account and that all material components are considered to have an elastic behaviour.

Concrete

In the beam element used in STANIL/1, concrete is subjected to a two-dimensional state of stress. In general, stresses σ_{xx}, σ_{yy} and σ_{xy} occur corresponding to deformations ε_{xx}, ε_{yy} and $2\varepsilon_{xy}$. The relation between an increment of stresses and an increment of strains may generally be described as:

$$\begin{bmatrix} \Delta\sigma_{xx} \\ \Delta\sigma_{yy} \\ \Delta\sigma_{xy} \end{bmatrix} = \begin{bmatrix} d_1 & d_2 & d_3 \\ d_4 & d_5 & d_6 \\ d_7 & d_8 & d_9 \end{bmatrix} \begin{bmatrix} \Delta\varepsilon_{xx} \\ \Delta\varepsilon_{yy} \\ \Delta 2\varepsilon_{xy} \end{bmatrix} \tag{7.1}$$

The coefficients d_1 to d_9 determine the stiffness of concrete against deformation. In STANIL/1 the following relations are used at present:

$$\begin{bmatrix} \Delta\sigma_{xx} \\ \Delta\sigma_{yy} \\ \Delta\sigma_{xy} \end{bmatrix} = \begin{bmatrix} E_x & 0 & 0 \\ 0 & E_y & 0 \\ 0 & 0 & G \end{bmatrix} \begin{bmatrix} \Delta\varepsilon_{xx} \\ \Delta\varepsilon_{yy} \\ \Delta 2\varepsilon_{xy} \end{bmatrix} \quad \textit{for uncracked concrete} \tag{7.2}$$

and if in one of the principal stresses, say direction 1, the tensile strength is exceeded:

$$\begin{bmatrix} \Delta\sigma_{11} \\ \Delta\sigma_{22} \\ \Delta\sigma_{12} \end{bmatrix} = \begin{bmatrix} 0 & 0 & 0 \\ 0 & E_2 & 0 \\ 0 & 0 & \alpha G \end{bmatrix} \begin{bmatrix} \Delta\varepsilon_{11} \\ \Delta\varepsilon_{22} \\ \Delta 2\varepsilon_{12} \end{bmatrix} \quad \textit{for cracked concrete} \tag{7.3}$$

The coefficients E_x, E_y and E_2 in the above relations are derived from the stress-strain diagram which is found by means of one-dimensional compression tests. The shear modulus G is taken as $0.5 \times E_0$, E_0 being the unit stiffness in the stress-straindiagram of concrete. In (7.3) α is a constant to simulate the aggregate interlock in cracked concrete. In STANIL/1 a default value is chosen, being $\alpha = 0.5$.

The tensile strength of concrete, i.e., the stress at which concrete will start cracking, is made dependent on the principal compressive stress in the two-dimensional state of stress (see Fig. 7.8).

The so called *tension stiffening effect* is taken into account. If cracks occur in reinforced concrete, the stress in the crack becomes zero, but a tensile stress may be transferred between two cracks. This phenomenon is taken into account for by adding a descending branch in the stress-strain diagram of concrete (in the tensile area). Crushing of concrete is assumed if strains occur in the structure which are smaller than ε_u (see Fig. 7.8).

Reinforcement and bond

Longitudinal reinforcement and stirrups are considered to be subjected to a one-dimen-

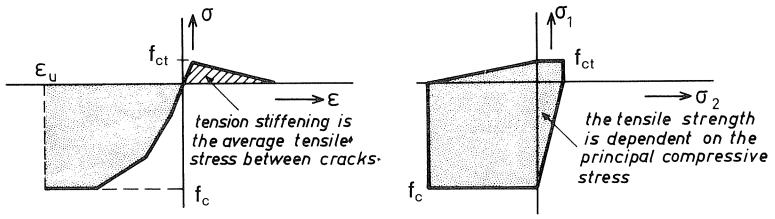

Fig. 7.8. The material properties of concrete are derived from a stress-strain diagram for one-dimensionnally loaded concrete and a crack/yield criterion for two-dimensionally loaded concrete.

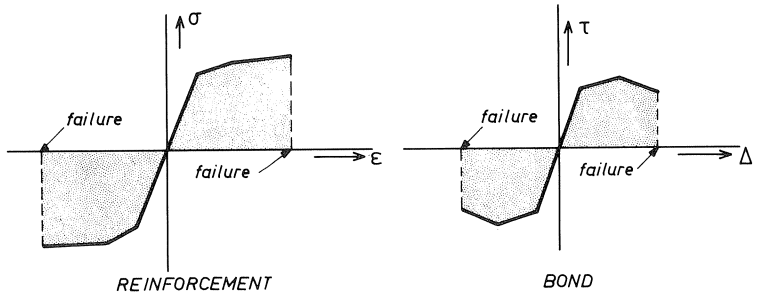

Fig. 7.9. The material properties of the reinforcement and bond are derived directly from the stress-strain and stress-slip diagram respectively.

sional stress situation in STANIL/1. Dowel action is not incorporated in the model. The relation between stresses and strains can therefore be derived directly from the relevant stress-strain diagram. The extreme values of the strains in the diagram are taken to be the failure criteria for the reinforcement (see Fig. 7.9).

For the bond between the longitudinal reinforcement and the surrounding concrete a similar assumption is made: the interaction takes place in a one-dimensional bond spring; there is a relation between the actual bond stress τ in the tubular surface of the spring and the actual bond slip Δ, the relative displacement of the reinforcement with respect to the surrounding concrete. The extreme slip values in the stress-slip relation are taken to be the failure criteria for the bond spring (see Fig. 7.9).

7.4 *Numerical procedure for nonlinear analysis*

The finite element method based on displacements yields a set of equilibrium equations which in matrix notation can be written as:

$$Sv - k = 0 \tag{7.4}$$

in which S represents the stiffness matrix of the structure, v the vector of displacements and k the load vector.

In case cracking of concrete is taken into account as described in section 7.3, the stiffness matrix S is a function of the actual strains and therefore a function of the displacements v. The set of equations in (7.4) is then nonlinear, characterized by a continuously changing coefficients matrix S. Therefore for solving (7.4) an iterative method is generally followed.

STANIL/1 offers the choice of two commonly used methods: the tangent stiffness method (also referred to as the Newton-Raphson method) and the initial stiffness method. In both methods the initial stiffness S_0 for the first iteration step is the same. From the second iteration step on, the tangent stiffness and the initial stiffness, respectively, are used in these two methods. The tangent stiffness method generally shows faster convergence, while the initial stiffness method has the advantage that the stiffness matrix has to be calculated and assembled only once, so that less computational effort is required for all iteration steps after the first. As it is often preferred to follow a load-deflection diagram step by step when performing a nonlinear analysis, an incremental procedure is incorporated in STANIL/1: the load may be applied in increments. For the iteration process this means that if the initial stiffness method is chosen in the STANIL/1 analysis, the method is applied per load increment. In a subsequent load increment a new initial stiffness is calculated for that increment.

Procedure

What actually happens in the iteration process consists in determining iteratively *those* displacements v for which (7.4) is satisfied. As an incremental procedure is followed in STANIL/1, it is more convenient to write (7.4) in terms of increments:

$$S_t \Delta v - \Delta k = 0 \tag{7.5}$$

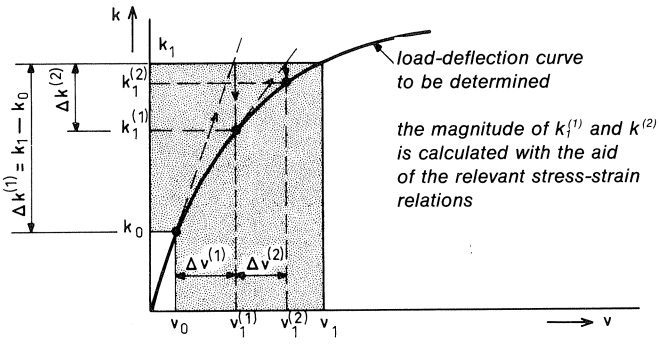

Fig. 7.10. Example of two iteration steps to determine the state of equilibrium k_1, v_1 starting from the state of equilibrium k_0, v_0 by the Newton-Raphson method.

in which Δv and Δk represent increments of nodal displacements and nodal forces respectively and S_t (a function of v) represents the tangent stiffness matrix. The iteration process is carried out with the aid of (7.5). The procedure will be discussed in more detail for the tangent stiffness method (Newton-Raphson).

Let us consider a structure in a state of equilibrium where the load on the structure is equal to $k = k_0$ and the corresponding actual displacements are equal to $v = v_0$. Next the load on the structure is increased to $k = k_1$ by applying a new load increment $(k_1 - k_0)$.

We now want to determine the displacements v_1 for which:

$$Sv_1 - k_1 = 0 \tag{7.6}$$

The first estimate $v_1^{(1)}$ for v_1 is made with the following linearized analysis (Fig. 7.10).

In the state of equilibrium k_0, v_0 we determine the (tangent) stiffness $S_t^{(0)}$. This is done as follows. The displacements v_0 correspond to strains. With the aid of the material properties the stiffness corresponding to the strains can be determined for each element of the structure and therefore also the stiffness matrix $S_t^{(0)}$ of the structure. The stiffness matrix $S_t^{(0)}$ is the tangent to the load-deflection diagram which we are looking for. Next we calculate the intersection point of this tangent with the line $k = k_1$ as follows:

$$\Delta k^{(1)} = k_1 - k_0 \tag{7.7a}$$

and

$$S_t^{(0)} \Delta v^{(1)} - \Delta k^{(1)} = 0 \tag{7.7b}$$

which yields $\Delta v^{(1)}$. The first estimate $v_1^{(1)}$ for v_1 is:

$$v_1^{(1)} = v_0 + \Delta v^{(1)} \tag{7.7c}$$

The displacements $v_1^{(1)}$ correspond to strains and the internal stresses which correspond to these strains can be derived from the relevant stress-strain relations. From the internal stresses, the internal nodal forces $k_1^{(1)}$ can be calculated. The new situation $v_1^{(1)}$, $k_1^{(1)}$

itself is a state of equilibrium again (though not one which was looked for) which serves as a starting point for a new estimate of v_1. The next iteration step is:

$$\Delta k^{(2)} = k_1 - k_1^{(1)} \tag{7.8a}$$

$$S_t^{(1)} \Delta v^{(2)} - \Delta k^{(2)} = 0 \rightarrow \Delta v^{(2)} \tag{7.8b}$$

$$v_1^{(2)} = v_1^{(1)} + \Delta v^{(2)} \tag{7.8c}$$

$$v_1^{(2)} \rightarrow k_1^{(2)} \tag{7.8d}$$

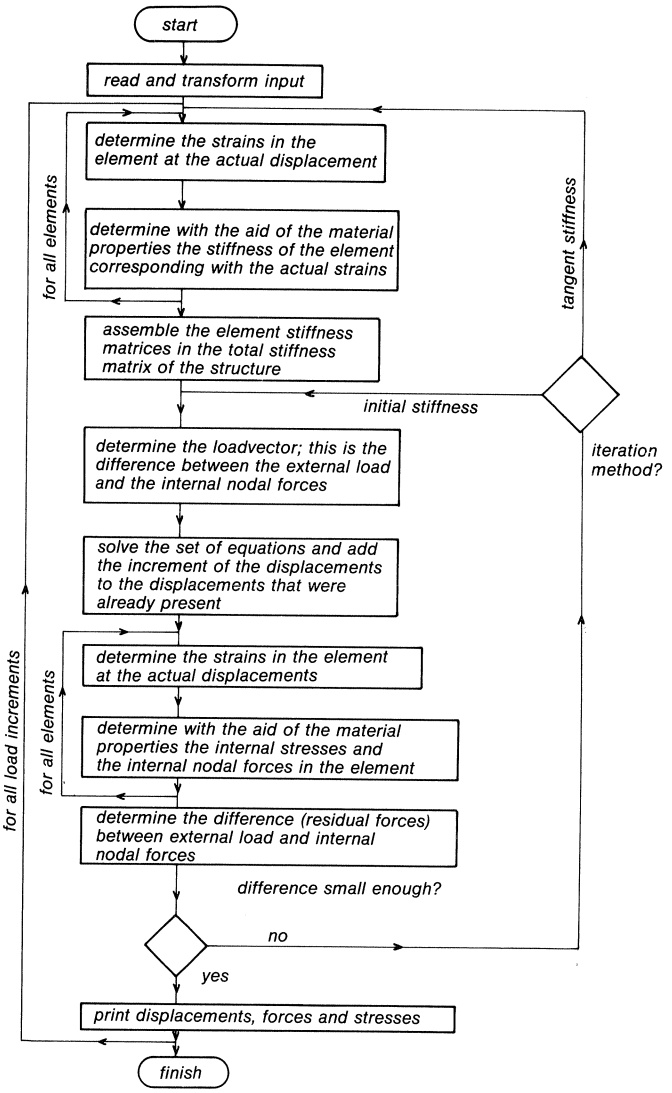

Fig. 7.11. Block diagram of the STANIL/1 program.

In general terms the iteration process can be written as:

$$\Delta k^{(i+1)} = k_1 - k_1^{(i)} \tag{7.9a}$$

$$S_t^{(i)} \Delta v^{(i+1)} - \Delta k^{(i+1)} = 0 \rightarrow \Delta v^{(i+1)} \tag{7.9b}$$

$$v_1^{(i+1)} = v_1^{(i)} + \Delta v^{(i+1)} \tag{7.9c}$$

$$v_1^{(i+1)} \rightarrow k_1^{(i+1)} \tag{7.9d}$$

This process is repeated until $\Delta k^{(i+1)}$ has become sufficiently small.

In the initial stiffness method the procedure is similar, but for all iteration steps after the first step of the load increment the stiffness matrix $S_t^{(i)}$ is not calculated again but taken as equal to $S_t^{(0)}$. The procedure followed in the STANIL program is indicated in Fig. 7.11.

8 Verification and application examples

In order to check the STANIL/1 program, an extensive verification was carried out. A number of limit cases was studied, such as beams subjected to respectively pure tension, pure bending and pure shear. Furthermore a study was carried out in which for one particular structure a number of parameters was varied, such as tensile strength of concrete, percentage of stirrup reinforcement, percentage of longitudinal reinforcement, etc. [15]. The object of this parameter study was to investigate the sensitivity of the STANIL/1 model to the variation of certain model parameters and also to check whether the behaviour predicted by STANIL/1 reflected the real behaviour, known from experiments. The results of the parameter study teach the following:

- The coefficient α for simulating the aggregate interlock has a weak influence.
- The tensile strength f_{ct} of concrete is of most importance. Only low values result in forming a truss in the beam.
- The bond characteristic for normal reinforcing bars hardly affects the behaviour of the beam.
- The anchorage zone spring has no influence.
- The percentage of main reinforcement is highly important. High percentages give rise to failure in shear. The shear strength increases if more main reinforcement is used.
- The effect of the percentage of web reinforcement on the behaviour of beams is considerable. For low values a truss will develop, and for high values a beam will fail in shear-compression.

Having checked the limit cases and the influence of the choice of model parameters, an analysis was carried out for some structures which have been investigated experimentally and in which the influence of shear was noticeable.

In this chapter, some results of analysis for the limit cases of pure bending and pure shear will be discussed. Furthermore, the results of analysis for a T-beam structure in shear and a continuous beam structure will be discussed and compared with experimental results.

8.1 *Beam subjected to pure bending*

One of the first verifications carried out with the STANIL/1 program concerned the case of pure bending. For this purpose, a structure for which material data and the moment-curvature diagram were known from experiments was analysed [10].

Calculations were done for three different values of tensile reinforcement, namely $\omega_0 = 1.50\%$, $\omega_0 = 0.50\%$ and $\omega_0 = 0.22\%$. Here we shall confine ourselves to the case: $\omega_0 = 0.50\%$. The cross-section of the beam is indicated in Fig. 8.1.

The stress-strain relation which was used for the STANIL/1 input is shown in Fig. 8.2. In the formula of Fig. 8.2 ε_{re} is the strain when the stress in the reinforcement reaches the yield stress; f_c is the compressive strength of the concrete measured at 28 days on cubes of $200 \times 200 \times 200$ mm^3 (in N/mm^2).

The stress-strain relation for the reinforcing steel was assumed to be bilinear with a slight round-off near the yield level. Inclusion of the slight round-off gives a smoother transition from the "cracked branch" in the moment-curvature diagram to the horizontal branch for yield.

The results of the STANIL/1 analysis together with the experimental results are shown in Fig. 8.3. In this diagram the bending moment is plotted as the ratio of the actual bending moment to the "ultimate" bending moment. The "ultimate" bending moment is taken as approximately equal to the bending moment when the reinforcement starts yielding in the experiment. It can readily be seen that the correlation between the experimental results and the STANIL/1 analysis is very good. Similarly good agreement has been obtained for other percentages of reinforcement. Both the stiffness of the structure involved and the ultimate failure load are predicted very well by STANIL/1.

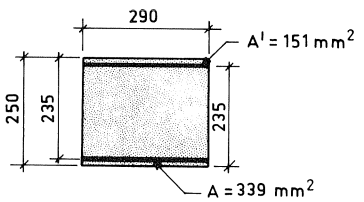

Fig. 8.1. Dimensions of the beam under investigation for pure bending.

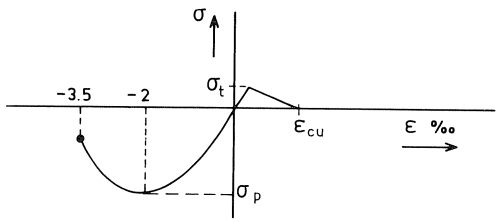

Fig. 8.2. The stress-strain relation of concrete used for the STANIL/1 input.

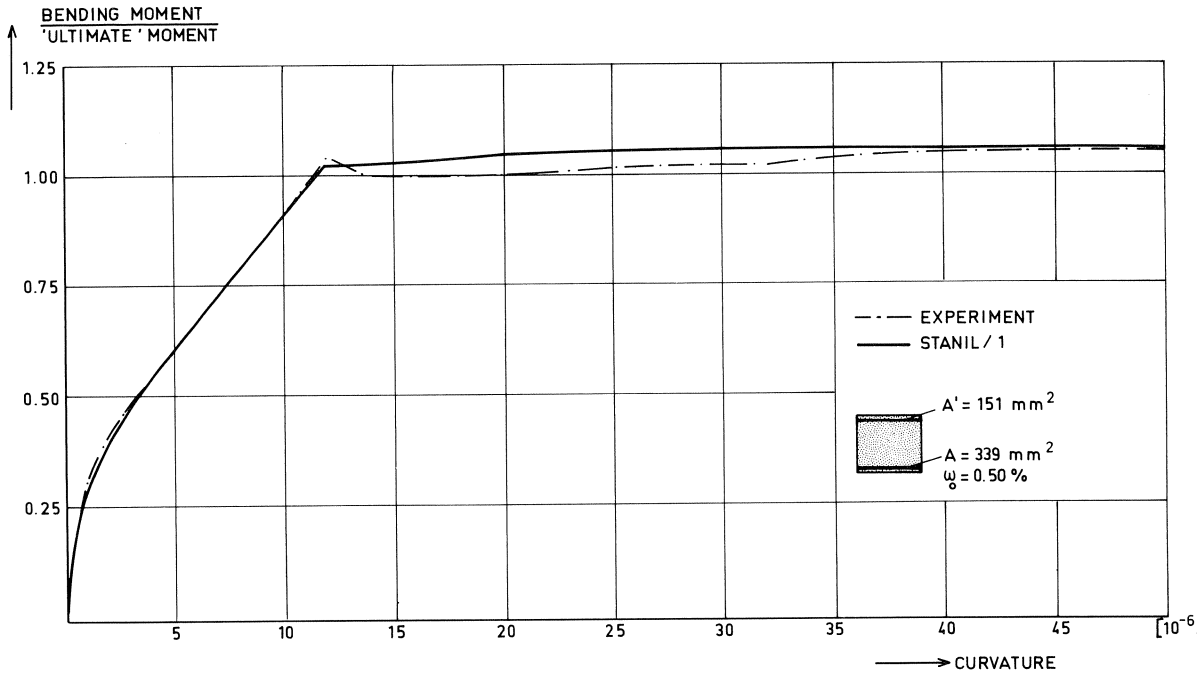

Fig. 8.3. The case of pure bending $\omega_0 = 0.50\%$.

8.2 *Beam subjected to pure shear*

The overall goal of the development of the new STANIL-beam model was to incorporate the effect of shear deformation in the model. It was already known that combinations of pure bending and axial forces could be simulated very well with the previous model. Including the effect of shear forces now, it was felt necessary to study thoroughly the behaviour of the model in the case where shear stresses are dominant. Therefore a *theoretical beam* was investigated.

The beam which was chosen (see Fig. 8.4) consists of infinitely rigid tensile and compressive flanges and a concrete web of finite rigidity. Due to the infinite rigidity of the flanges, the axial strains in the concrete web will remain zero. As long as no cracking occurs, no vertical stresses will occur either. Just a state of constant shear stress is present in the web. Once diagonal cracks occur (initially under 45°), internal redistribution of stresses will take place, after which vertical stresses will occur in the concrete, due to action of the stirrups (tension in the stirrups, compression in the concrete). Calculations were carried out with STANIL/1 for several amounts of web reinforcement, corresponding to ω-values 0.025, 0.05, 0.1, 0.2 and 0.6, where ω is the mechanical proportion of stirrup reinforcement which is defined as $\omega = \rho f_y / f_c$ in which ρ is the percentage of stirrup reinforcement, f_y the yield strength of the stirrup steel and f_c the yield strength of concrete. The coefficient for simulating the aggregate interlock of cracked concrete was assumed to be $\alpha = 0.5$.

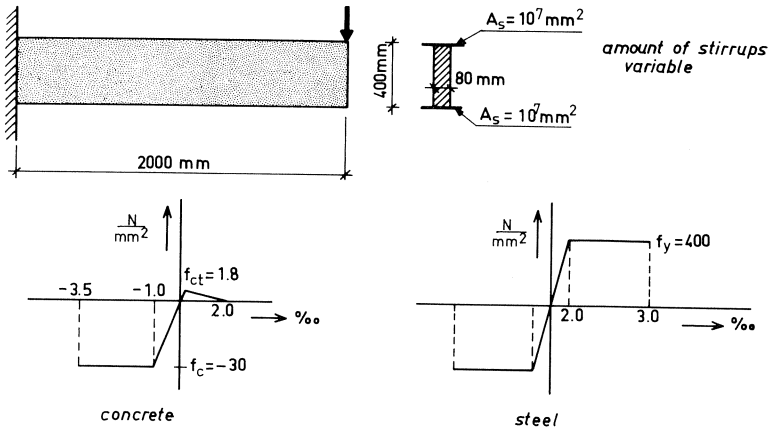

Fig. 8.4. Dimensions and material properties of the beam under investigation for pure shear.

A typical result is shown in Fig. 8.5. This is the load-deformation curve for the case $\omega = 0.1$. The model can describe a number of aspects:

- The initial crack inclination of 45° changes with increasing load.
- The ultimate failure load predicted by STANIL/1 corresponds very well to the failure load predicted by a theory of plasticity for the same theoretical beam model (Nielsen et al.).

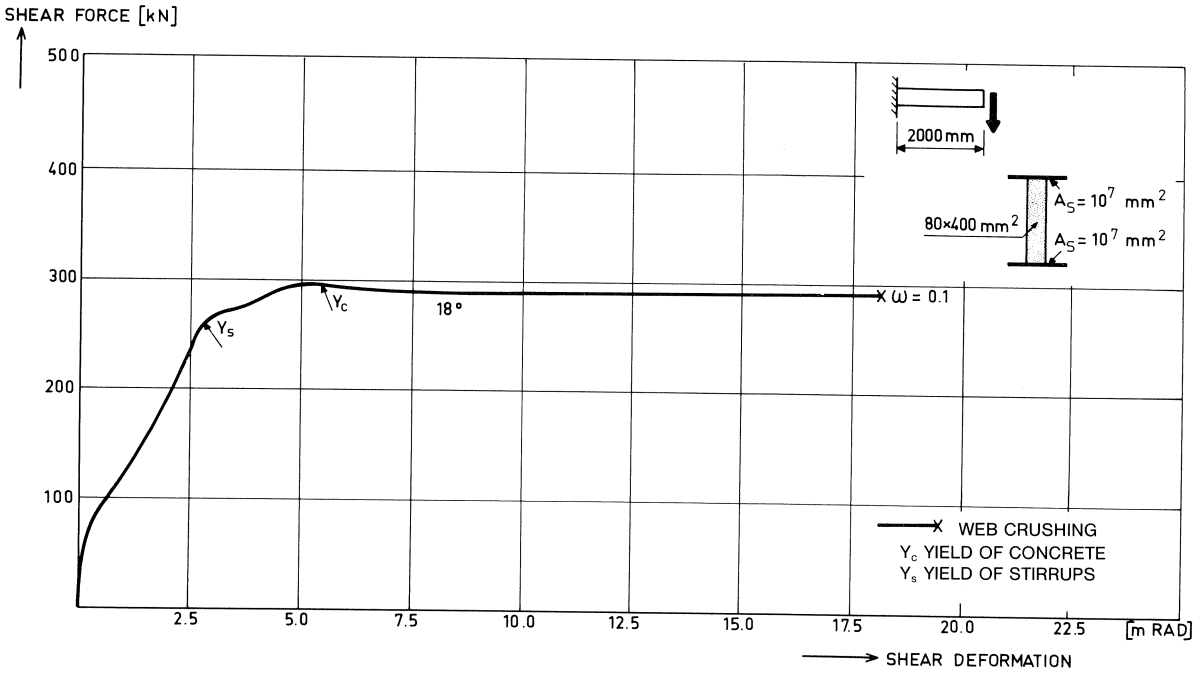

Fig. 8.5. Load-deformation curve for the case of pure shear.

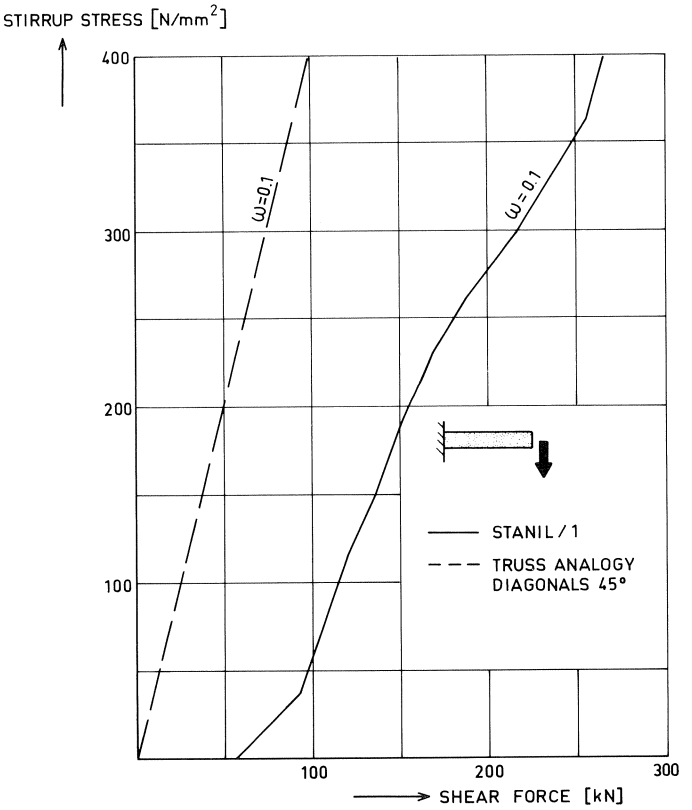

Fig. 8.6. The relation between stress in stirrups and shear force for the case of pure shear.

- At failure load the web may crush and/or the stirrups yield. STANIL/1 predicts the same phenomena as the plasticity approach of Nielsen et al. For very low percentage of stirrups the STANIL/1 program provides additional information. The strains in the stirrups then become so large that they may be considered to fracture.

Another interesting result which can be obtained with a STANIL/1 analysis is shown in Fig. 8.6. Here the stresses in the stirrups are plotted versus the applied shear force for ω-value of 0.1. Furthermore the dashed line indicates the relation which would apply if the truss analogy would hold with bars inclined at 45° and zero tensile concrete strength.

The results qualitatively reflect the behaviour which is known from experiments: a certain amount of shear force can be resisted without the stirrups being stressed; first after diagonal cracking of the concrete the stresses in the stirrups increase roughly with a similar steepness as predicted by truss analogy (the dashed line).

8.3 *Shear test on a T-beam*

In Section 8.2 we examined a theoretical beam in pure constant shear. In order to inves-

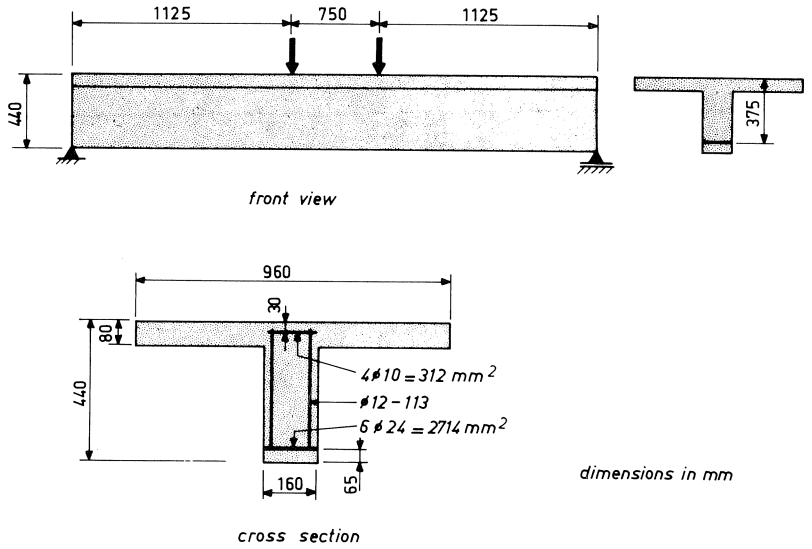

Fig. 8.7. Survey of the structure; shear test on a T-beam.

tigate whether the STANIL/1 beam model is able to predict reasonably the behaviour of realistic structures in which shear deformations are considerable, a beam was analysed for which Leonhardt and Walther published material data and experimental results in [16].

The experiment consisted of a simple test on a beam which had a T-shaped cross section; the beam was referred to as TA1. The structure is shown in Fig. 8.7. In this beam no homogeneous state of shear stresses is to be expected.

In the STANIL/1 analysis only half the structure was considered because of symmetry. A total of 4 beam elements was used, each 375 mm long (3 in the shear span, 1 in the constant moment area). In the experiment the structure was loaded by applying two point loads which were increased step by step. In the STANIL/1 analysis a displacement controlled approach was used. Instead of applying a point load, the displacement of that point of the beam was increased incrementally.

The load displacement curve of the structure is shown in Fig. 8.8. It is to be noted that for shear forces higher than 300 kN no experimental data are available. The ultimate failure that was measured in the test was equal to 348 kN while the STANIL/1-analysis gave 343 kN. It can therefore be concluded that both the failure load and the global stiffness of the structure as predicted by STANIL/1 show very good correlation with the experimental data.

Furthermore the failure mode found in the STANIL/1-analysis (web crushing), was also indicated in the test report. It is also worth noting that the STANIL/1-analysis predicts limited ductility for the structure. The test report also contains data on the stresses in the stirrups. In Fig. 8.9 a comparison of the test results is made with the results of the STANIL/1-analysis.

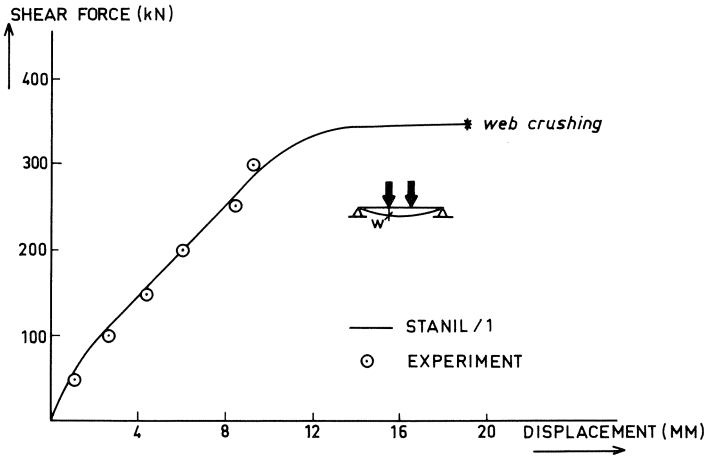

Fig. 8.8. Load-displacement diagram, shear test on a T-beam.

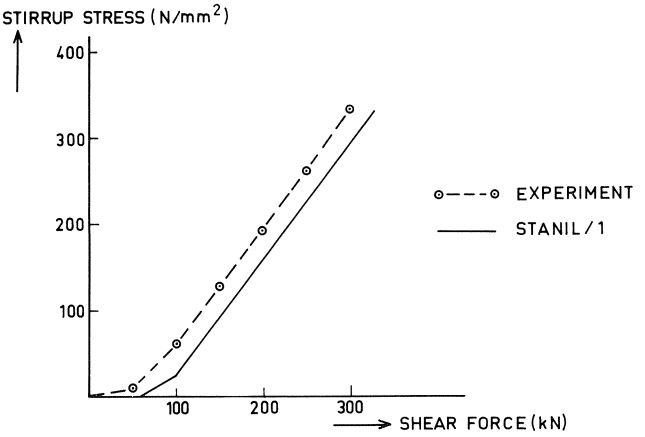

Fig. 8.9. The relation between the stresses in the stirrups and the applied shear force; shear test on a T-beam.

The correlation between the STANIL/1 results and the experimental results is fairly good. This becomes even more clear on considering that the experimental curve was found by averaging the stresses of four stirrups which showed higher stresses than the average of the total shear span. On the other hand, the stresses in the stirrups as predicted by STANIL/1 were practically the same in all three elements in the shear span.

8.4 *Continuous beam structure*

A further expansion of the investigation of the capabilities of the STANIL/1 beam model concentrated on a continuous beam structure being supported at three places; experimental results for the beam under investigation were reported in [17]; the beam

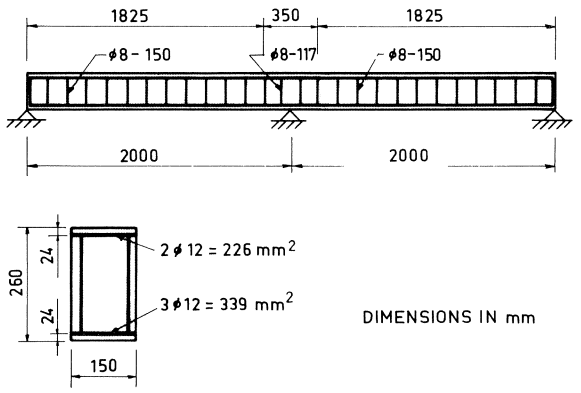

Fig. 8.10. Survey of the structure; continuous beam structure.

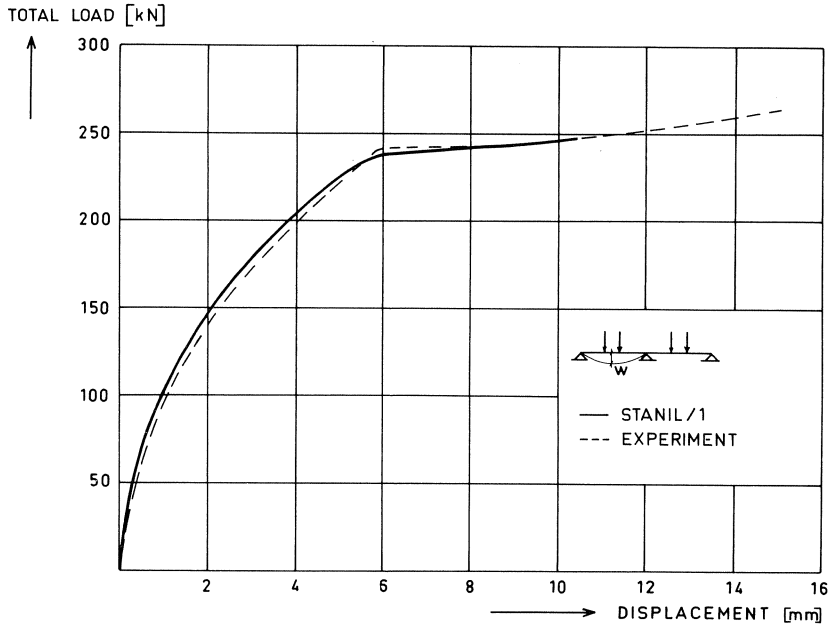

Fig. 8.11. Load-displacement curve; continuous beam structure.

was referred to as beam B2. The test beam was designed such, that the effect of shear forces on the stiffness of the beam after cracking may not be neglected. The beam under investigation is shown in Fig. 8.10.

In the STANIL/1 analysis only half the structure was considered because of symmetry. A total of 8 beam elements, each 250 mm long, was used. The material properties were taken from [17].

In the experiment as well as in the STANIL/1 analysis the load was increased step by step. The load-displacement curve of the structure is shown in Fig. 8.11.

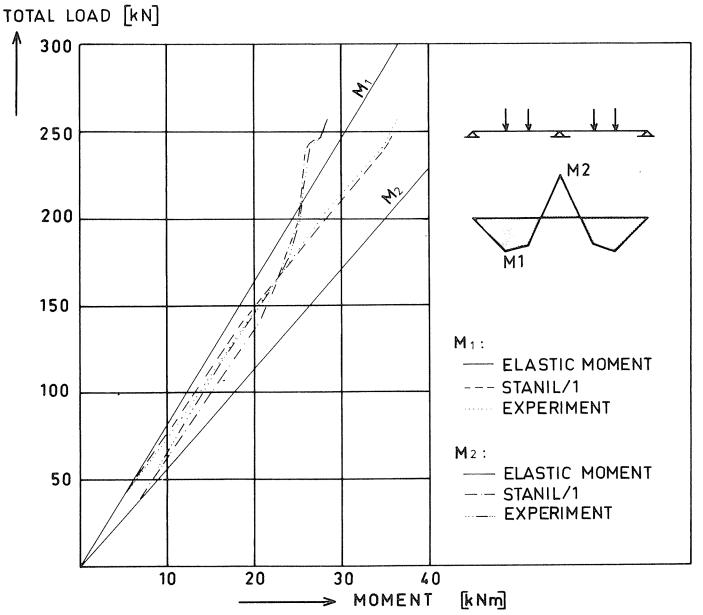

Fig. 8.12. Bending moments in the span and at the middle support for varying load; continuous beam structure.

It may be concluded that the correlation between the results of the STANIL/1 analysis and the experimental results is very good. This is particularly interesting as it was shown earlier, that with a beam element, not accounting for shear deformation, it was not possible to analyse this structure properly. Apparently the extension of the element with shear deformation as described in this report increases the capability of the element considerably.

In the experiment, the maximum bending moment in the span and the bending moment at the support in the middle, were also recorded during the loading of the structure. The results of the experiment are compared with those of the STANIL/1 analysis in Fig. 8.12.

Once more, it is apparent that the correlation between STANIL/1 results and experimental results is good. It may therefore be concluded that the STANIL/1 beam model is very well capable of simulating the behaviour of this continuous beam structure.

9 Conclusions and work ahead

The STANIL/1 program is an extension and renewal of the existing program STANIL on the basis of "smeared-out" material properties. The old program was capable of handling deformations due to extension and to bending, and combinations thereof. Geometrical nonlinearities were taken into account. The materials were defined in non-

linear elastic terms and a tension-stiffening feature was implemented. In the old program only cracks normal to the bar axis could occur, either over a part of the depth of the beam or all-through cracks.

The extension introduced in the newly derived program STANIL/1 comprises, apart from additional options, the possibilities to allow for shear deformation and to model the bond mechanism between the main reinforcement and the concrete. Now crack patterns may occur which are inclined to the bar axis.

Conclusions

Fully in accordance with its ultimate purpose the Macro-model is capable of dealing with shear deformations and bond slip, while the correct simulation of pure bending and pure tension and combinations thereof and the geometrical nonlinearity are preserved. The prediction of crack patterns in the web of girders is satisfactory, as well as the feature that the inclination of shear cracks changes for increasing load. In a case where the deflection of a beam is due to both bending deformation and shear deformation, the analysis with the new STANIL/1 program shows better results than the old STANIL program.

The results found for the stresses in the stirrups are in agreement with existing experience and expectations. For a main reinforcement percentage as normally applied in practice, the bar does not slip relative to the concrete. The stiffness of the bond spring (if not chosen extremely small) is of no marked influence on the results. If inclined shear cracks occur, the stress in the main reinforcement is increased by a constant amount along that part of the beam where a constant shear force occurs. This conforms to what can normally be expected.

Conceptually, the Macro-model has not been derived to investigate detailed stresses but to determine the global behaviour of a beam or framed type structure in a reliable way. This aim has indeed been achieved, which implies at the same time that we are prepared to accept a less sound representation of the full internal state of stress.

Work ahead

There are always possibilities for improving a numerical model. In the case of the Macro-model one may for instance think of a special element for the beam-to-column connection. In Section 4.4 the Micro-model application gave information on the cracking and slip aspects in such an area. In Chapter 6, however, it has been stated that the Macro-model presupposes perfectly rigid connections. Therefore a special element would be advisable.

In any case one can implement the results of project 1 and 2 of "Betonmechanica" in the Macro-model. The force transfer study of project 1 should result in a more general constitutive relation for (reinforced) cracked concrete than has been tentatively chosen in MACRO/1 for the time being. The bond model can be made more realistic, too, taking account of the effect of radial stresses as well (which now has been neglected).

However, in view of the weak influence of the bond layer properties on the global behaviour, an adaption of the bond layer is not very urgent.

A desired feature in STANIL/1 is the implementation of creep and shrinkage. It will have to be judged in the future if such an extension is sufficiently attractive and worthwhile.

Finally, a major task is seen in so extending the Macro-model that frames in three-dimensional space can be analysed. This involves bending and shear deformation in two different planes and, apart from extensional deformation, also a torsional deformation mode. The connections in such space-frames will be of even greater complexity.

References

1. Workplan and survey of Betonmechanica, 1977.
2. WALRAVEN, J. C. and H. W. REINHARDT, Theory and experiments on the mechanical behaviour of cracks in plain and reinforced concrete subjected to shear loading. Heron, 1981, nr. 1a.
3. GROOT, A. K. DE, G. M. A. KUSTERS and TH. MONNIER, Numerical modelling of bond-slip behaviour. Heron, 1981, nr. 1b.
4. GROOTENBOER, H. J., Finite element analysis of two dimensional reinforced concrete, taking account of nonlinear physical behaviour and development of discrete cracks, Doctoral thesis, Delft University of Technology, The Netherlands, March 1979.
5. LEIJTEN, S. F. C. H. and J. BLAAUWENDRAAD, Stanil/1, a macro-beam-model for the nonlinear analysis of reinforced concrete plane frames. Rijkswaterstaat, February 1981.
6. BLAAUWENDRAAD, J., Systematical derivation of direct methods and variational principles for continuum and discrete models in solid mechanics (in Dutch). Doctoral thesis, Delft University of Technology, 1973.
7. LINK, J., Eine Formulierung des zweiaxialen Verformungs- und Bruchverhaltens von Beton und deren Anwendung auf die wirklichkeitsnahe Berechnung von Stahlbetonplatten. Deutscher Ausschuss für Stahlbeton, Heft 270, Berlin 1976.
8. BUYUKOZTURK, C., Nonlinear analysis of reinforced concrete structures. Computer & Structures, Vol. 7, No. 1, Febr. 1977, pp. 149–156.
9. CEB, Système international de reglementation technique unifiée des structures. Bulletin d'information No. 111, October 1975.
10. MONNIER, TH., The moment-curvature relation of reinforced concrete. Heron, Vol. 17, 1970, No. 2.
11. LEONHARDT, F. and R. WALTHER, Wandartige Träger, Deutscher Ausschuss für Stahlbeton, Heft 178, Berlin 1966.
12. WALRAVEN, J. C., The influence of depth on the shear strength of lightweight concrete beams without shear reinforcement. Report 5-78-4, Delft University of Technology, Stevin Laboratory, 1978.
13. HOEKSTRA, A. S., The influence of the detailing of reinforcement on the behaviour of the continuous beam-to-column connection, Delft University of Technology, Civil Eng. Dept. 1977 (in Dutch).
14. BLAAUWENDRAAD, J., Realistic analysis of reinforced concrete framed structures. Heron, Vol. 18, 1972, No. 4.

15a. MIER, J. G. M. VAN, Parameter study with the Macro-beam-model, CUR-Report A26/79-04, 1979 (in Dutch).

b. LEIJTEN, S. F. C. H. and J. G. M. VAN MIER, Addendum to the CUR-Report A26/79-04, CUR-Report A26/79-04a, 1980 (in Dutch).

16. LEONHARDT, F. and R. WALTHER, Schubversuch an Plattenbalken mit unterschiedlicher Schubbewaehrung, Berlin, Deutscher Ausschuss für Stahlbeton, Heft 156, 1963.
17. MONNIER, TH., The behaviour of continuous beams in reinforced concrete. Heron, Vol. 17, 1970, No. 1.